TOPICAL REPORT

ANALYTICAL STUDY OF LIQUID METAL
CONDENSING INSIDE TUBES

prepared for
National Aeronautics and Space Administration

January 1965

Contract NAS3-2335

Technical Management
NASA Lewis Research Center
Space Power System Division
Nuclear Power Technology Branch
Cleveland, Ohio
Martin Gutstein

Written by _____ H.R. Kunz, Project Engineer

Approved by _____ S.S. Wyde, Program Manager

_____ W.J. Lueckel, Chief, Space
Power Systems

Pratt & Whitney Aircraft DIVISION OF UNITED AIRCRAFT CORPORATION

E A S T   H A R T F O R D   ●   C O N N E C T I C U T

FOREWORD

This report was prepared by the Pratt & Whitney Aircraft Division of
United Aircraft Corporation, East Hartford, Connecticut, to describe
the work conducted from May 15 to December 1, 1964 in fulfillment
of Task IV of Contract NAS3-2335, Experimental Investigation of
Transients in Simulated Space Rankine Powerplants, Amendment 4.
The report summarizes an analytical study of condensing flow inside
tubes. Some of the material generated in this study is being used by
the author as part of a doctoral thesis at Rensselaer Polytechnic
Institute in Troy, New York.

The author wishes to acknowledge assistance provided by S.S. Wyde,
H.L. Hess, and H.L. Ornstein in computer programming and
report editing.

TABLE OF CONTENTS

LIST OF FIGURES

I. SUMMARY

24013 *ABST*

An analysis is presented of annular, two-phase flow inside of circular tubes. This analysis enables an estimation of the liquid film thickness for one or two-component flow and the heat transfer coefficient for condensing flow of a pure fluid. Special consideration is given to condensing liquid metals.

Results obtained using this analysis were found to be in good agreement with measured values of liquid film thickness in vertical upflow and downflow for air-water mixtures in annular adiabatic flow. Similarly, condensing heat transfer coefficients calculated for vertical downflow of steam were found to be in good agreement with measurements. Finally, results of sample calculations are presented for condensing potassium. These results indicate that if no liquid-vapor interfacial resistance to heat flow is considered, the local values of condensing coefficients for potassium in vertical downflow inside a tube are higher than those calculated using Nusselt's theory for laminar condensing on a vertical surface with no liquid-vapor interfacial shear. This interfacial resistance to heat flow could result in significant reductions in heat transfer coefficients for condensing potassium.

In the analytical approach, all liquid is considered to be flowing in an annular film along the tube wall with no liquid entrainment in the vapor core. Shear stress and heat flux distributions are derived for the liquid film and are combined with empirical expressions for turbulent diffusion coefficients and wall shear stress to enable calculation of the liquid velocity and temperature profiles. The expressions for turbulent diffusion coefficients are obtained from data for fully-developed single-phase pipe flow. The velocity and temperature profiles enable the liquid film thickness and condensing heat transfer coefficients to be determined. No adjustment of empirical constants obtained from single-phase data was necessary to obtain agreement between theory and two-phase data.

Author

II. INTRODUCTION

From July to December 1963, an analytical design study was conducted by Pratt & Whitney Aircraft on shell-and-tube condensers for use as one of the compact condensers of a one megawatt (electric) nuclear Rankine cycle space powerplant[1]. This study indicated that insufficient experimental and theoretical information was available concerning condensing heat transfer coefficients and liquid holdup in condenser tubes. This information may be required for condenser design and for determination of the variation of system fluid inventory with operating conditions for any given design. Because of the above-mentioned deficiency in theoretical information, an analysis of condensing flow inside of tubes was conducted. This report presents the results of that study.

The report begins with a brief review of the theoretical and experimental work conducted for the determination of the condensing heat transfer coefficients for flow inside of tubes where the condensate film is in turbulent flow. The primary assumptions of each of these theoretical approaches are indicated and the derivation of the new method is presented. This new analysis removes most of the assumptions which are inadequate for condensing liquid metals flowing inside of tubes. The final equations of this analysis were programmed on a digital computer* in order to rapidly calculate liquid film thickness and condensing coefficients. Comparisons of theoretical values are made in this report with available data for conventional fluids. Finally, estimates are presented for the condensing heat transfer coefficients for potassium.

---

[1]Numbered references are listed in Appendix E.

*Copies of a manual describing this computer program, Report NASA CR-54350, are on file at the NASA office of Scientific and Technical Information, Washington 25, D.C.

III. PREVIOUS APPROACHES

A large number of papers have been published treating the condensation on vertical flat plates and inside vertical tubes where the liquid condensate film is in laminar flow. This literature is not reviewed in this report but is discussed in many heat transfer texts. Condensation with a turbulent film was first treated by Colburn[2]. He derived a semi-theoretical relationship for predicting heat transfer coefficients for turbulent condensate flow, considering that transition from laminar to turbulent flow occurs at a film Reynolds number of 2100 and liquid-vapor interfacial shear is absent. In a later study, Carpenter and Colburn[3] included the effects of interfacial shear and momentum transport at the liquid-vapor interface due to the mass transfer, as well as the effects of gravitational force and wall force. The shear stress at the liquid-vapor interface was obtained from a correlation derived by Bergelin, et al[4]. The assumption was made that the only resistance to heat flow is due to the viscous sublayer of the condensate flow and that this layer is of constant dimensionless thickness ($y v*/ v_L$ at edge of viscous sublayer = constant). This approach led to fair agreement between theory and data for a number of conventional fluids in turbulent condensing vertical down-flow inside a tube.

Seban[5], Rohsenow, et al[6], and Altman, et al[7] included the effects of the resistance of the turbulent portion of the film in addition to the resistance of the viscous sublayer. All of these approaches used the universal velocity profile for turbulent flow to determine the turbulent eddy diffusion coefficients for momentum. The assumption was made in these approaches that the turbulent eddy diffusion coefficients for heat equals that for momentum, thereby enabling the temperature profile across the liquid layer to be calculated. This approach was first used by Martinelli[8] for fully-developed single-phase flow. In order for these approaches to apply to condensing inside a tube, all of the liquid must flow in an annulus along the inside of the tube wall. Seban assumed no interfacial shear. Rohsenow, et al considered that the interfacial shear can be calculated using the correlation of Bergelin, et al[4]. Altman, et al assumed that the wall shear stress could be calculated from the adiabatic pressure loss correlation of Martinelli and Nelson[9]. All of these methods showed good agreement with appropriate data for conventional fluids.

Dukler[10] presented an analysis similar to that used by Deissler[11]
for fully-developed turbulent pipe flow. In this approach a shear
stress distribution was calculated across the liquid film ignoring
the effect of static pressure forces in the film. Wall shear stress
was calculated from an empirical correlation for adiabatic two-phase
vertical downflow. The heat flux was assumed to be constant across
the liquid film. The film was divided into two regions and appropriate
expressions for eddy diffusion coefficients were used in each region.
The ratio of eddy diffusion coefficient of heat to that of momentum
was assumed to be equal to one and molecular conduction was neglect-
ed in the region away from the wall. The results of this analysis
agreed very well with measured film thickness in adiabatic downflow
and condensing coefficients for conventional fluids in vertical down-
flow inside a tube.

All of the above methods involve assumptions which make them in-
adequate for the determination of the condensing coefficients for liquid
metals. For condensing liquid metals, the resistance of the entire
condensate layer must be included because of the low Prandtl number
of such fluids. In addition, the ratio of eddy diffusion coefficients
is probably not equal to one, particularly in a thin condensate layer
in close proximity to a wall. Also, frictional, gravitational and static
pressure forces due to condensation should be included in the mo-
mentum equation for a fluid element in the liquid layer.

In addition to the resistance to heat flow caused by the liquid layer,
interfacial thermal resistances between the liquid and the solid wall
and between the vapor and the liquid may be present in liquid metals.
Kirillov, et al[12] found that wall-liquid interfacial resistances can be
present in single-phase alkali metal systems but can be eliminated by
adequate removal of oxygen. Sukhatme and Rohsenow[13] have indicated
that significant vapor-liquid interfacial resistances can be present
due to the high heat flux rates present in liquid metal condensation.
They found this resistance present in mercury condensation.

Little data is available for liquid metal condensing. Misra and
Bonilla obtained data for condensing mercury and sodium on a verti-
cal surface. This data indicated condensing heat transfer coefficients

much lower than those predicted by Seban's theory. Chen[15] and Lee[16] suggested that this disagreement may be due to upward vapor shear on the liquid condensate layer. Rohsenow suggested that it is due to vapor-liquid interfacial resistance to heat flow. Condensing heat transfer coefficients for potassium flowing downward inside a vertical tube were obtained by Sawochka[17]. This data also indicates measured values much lower than those predicted by Seban's theory.

Because of the disagreement between presently available theories and data, more experimental and theoretical work is required in the area of liquid metal condensation. The purpose of this study is to present an analysis of the condensate layer resistance which includes additional factors not considered by previous investigations and which therefore would be more applicable for liquid metals. The estimates of this resistance can be used for design purposes. Also, the presence and magnitude of additional resistances such as liquid-vapor interfacial resistance can be more accurately determined from experimental liquid metal data. Since the present approach also yields estimates of liquid film thickness, estimates of fluid inventory will also result.

IV. THEORY

The physical problem to be analyzed is that of two-phase liquid-vapor
flow inside a tube in which the liquid flows in an annular layer along
the wall and the vapor flows in the core. This flow pattern is gen-
erally present in condensing tubes in which the flow direction is
vertically downward and is anticipated to be the flow regime present
in condensers in zero gravity. In addition, this flow pattern is common
in two-phase two-component flow, including the case of vertical upflow.
Therefore, the vapor in this analysis is considered to consist either of
the same substance as the liquid or a different substance to make the
analysis more general. For the former case, the condensing heat
transfer coefficient and liquid layer thickness at a local axial position
are desired as a function of tube diameter, fluid, quality, pressure,
flow rate, heat removal rate from the tube, gravity field, and tube
orientation. In the latter case, the thickness of the liquid layer is
desired as a function of the tube diameter, fluids, fluid flow rates,
pressure, temperature, gravity field, and tube orientation. The
thickness of the liquid layer enables the amount of liquid present in
the tube to be determined. Single-phase flow is a limiting case of
these two-phase flow cases in which the core flow is considered to be
zero.

The basic approach to the problem is to determine the thickness of
the liquid film by determining the velocity distribution across this
film, and then to determine the temperature distribution across the
film to obtain the local heat transfer coefficient.

The major assumptions are:

    1)   The liquid film is annular and axisymmetric (see Figure 1,
          Appendix F).
    2)   Only gas or vapor is present in the core.
    3)   The flow is steady.
    4)   Condensing mass transfer occurs at the liquid-vapor
          interface.
  *5)   Liquid properties are assumed constant across the film.
  *6)   Sensible heat due to liquid subcooling is negligible.
    7)   The eddy diffusion coefficients of momentum and heat are
          obtainable from empirical equations.

8)   The wall shear stress is obtainable from correlations of
     two-component, adiabatic pressure loss data.
*9) The acceleration terms can be neglected in the momentum
     equation of the liquid layer.
10) The static pressure is uniform across the tube.
*11) Momentum fluxes can be evaluated using flow average
     velocities.
12) The vapor is at saturation temperature.

The velocity and temperature profiles across the liquid film are
obtained from the transport equations for turbulent flow which are:

$$\tau = \frac{1}{g_c} \left(\mu_L + \rho_L \, \epsilon_M \right) \frac{du}{dy} \tag{1}$$

$$q = -\left(k_L + \rho_L \, C_{P_L} \, \epsilon_H \right) \frac{dt}{dy} \tag{2}$$

These equations account for the transport for momentum and energy
through the action of both molecular and turbulent transport
mechanisms.

Dividing Equation (1) by the shear stress at the wall τ_0, and Equa-
tion (2) by the heat flux at the wall q_0 the following equations are
obtained

$$\frac{\tau}{\tau_0} = \frac{1}{\tau_0 \, g_c} \left(\mu_L + \rho_L \epsilon_M \right) \frac{du}{dy} \tag{1a}$$

$$q/q_0 = -\frac{1}{q_0} \left(k_L + \rho_L C_{P_L} \, \epsilon_H \right) \frac{dt}{dy} \tag{2a}$$

*Not applicable to cases for adiabatic fully-developed flow

Multiplying and dividing by $\mu_L \rho_L$, and rearranging terms

$$\frac{\tau}{\tau_0} = \frac{\mu_L \, \rho_L}{\tau_0 g_c \, \rho_L} \left(1 + \frac{\rho_L}{\mu_L} \epsilon_M \right) \frac{du}{dy} \qquad (1b)$$

$$\frac{q}{q_0} = - \frac{C_{P_L} \, \mu_L \, \rho_L}{q_0 \, \rho_L} \left(\frac{k_L}{C_{P_L} \mu_L} + \frac{\rho_L}{\mu_L} \epsilon_H \right) \frac{dt}{dy} \qquad (2b)$$

Noting that $\dfrac{C_{P_L} \, \mu_L}{k_L} \equiv Pr_L$, $\dfrac{\mu_L}{\rho_L} \equiv \nu_L$, $\sqrt{\dfrac{\tau_0 \, g_c}{\rho_L}} \equiv v*$ and

$\dfrac{\epsilon_H}{\epsilon_M} \equiv \alpha$ the equations can be written as:

$$\frac{\tau}{\tau_0} = \frac{\nu_L}{(v*)^2} \left(1 + \frac{\epsilon_M}{\nu_L} \right) \frac{du}{dy} \qquad (1c)$$

$$\frac{q}{q_0} = - \frac{C_{P_L} \, \nu_L \, \rho_L}{q_0} \left(\frac{1}{Pr_L} + \alpha \frac{\epsilon_M}{\nu_L} \right) \frac{dt}{dy} \qquad (2c)$$

Defining the dimensionless variables

$$u+ \equiv \frac{u}{v*} , \qquad y+ \equiv \frac{y \, v*}{\nu_L} , \qquad t^+ \equiv \frac{C_{P_L} (t_0 - t) \rho_L \, v*}{q_0}$$

and noting that $\dfrac{dt^+}{dy^+} = \left(\dfrac{-C_{P_L} \, \rho_L \, \nu_L}{q_0} \right) \dfrac{dt}{dy}$ and $\dfrac{du^+}{dy^+} = \dfrac{\nu_L}{(v*)^2} \dfrac{du}{dy}$

the transport equations can be written in the following forms

$$\frac{\tau}{\tau_0} = \left(1 + \frac{\epsilon_M}{\nu_L} \right) \frac{du+}{dy+} \tag{1d}$$

$$\frac{q}{q_0} = \left(\frac{1}{Pr_L} + \alpha \frac{\epsilon_M}{\nu_L} \right) \frac{dt^+}{dy+} \tag{2d}$$

An empirical expression of van Driest[18] is used for the eddy diffu-
sivity of momentum

$$\frac{\epsilon_M}{\nu_L} = K^2 y^{+2} \left[1 - e^{-y^+/A^+} \right]^2 \frac{du^+}{dy}+ \tag{3}$$

This expression has been found to lead to good estimates of heat
transfer coefficients in single-phase flow.

Van Driest's expression for eddy diffusion coefficients was obtained
by an extension of Prandtl's mixing length approach to include
viscous damping of turbulent eddies near a wall. Empirical constants
in this expression were obtained from velocity profiles in fully-
developed pipe flow in the region near the wall. The constant K was
found to equal 0.40 and A^+ was found to equal approximately 26.
Far from the wall, this expression provides values of diffusion co-
efficient which are in error. However, since the diffusion coefficient
is very high in that region, the velocity profile is affected only very
slightly by such incorrect values of ϵ_M / ν_L . For the case of a con-
densing film, in which shear stress distributions may go to zero at
the liquid-vapor interface, van Driest's expression can be seen to
permit zero values of eddy diffusion coefficient at the liquid-vapor
interface. Since this occurrence is considered unrealistic, an alter-
nate option to using van Driest's equation is provided in the analysis.
This option uses Van Driest's expression out to the distance from the
wall at which a maximum value of turbulent diffusion coefficient

occurs. For greater distances from the wall, the option considers the diffusion coefficient to be constant and at its maximum value. This option was used for the calculations of all results presented in this report. The validity of this assumption for single-phase flow is shown in Figure 2, where the velocity profile for single-phase flow calculated using this method and the present analysis are compared with the universal velocity profile which has been fitted to the data of Laufer[19]. The calculated distributions of shear stress and turbulent diffusion coefficient of momentum are also shown in Figure 3. The Reynolds number used for these calculations corresponds to one of those of Beckwith and Fahien[20], who obtained data on the ratio of eddy diffusion coefficients of heat and momentum. The latter data will be discussed later in this report.

In the study of heat transfer to liquid metals in single-phase fully-developed turbulent flow inside tubes, a number of investigators[21, 22, 23, 24, 25, 26, 27, 28] have derived expressions for α, the ratio of eddy diffusion coefficient of heat to that of momentum. All of these studies considered that conduction of heat occurred between a turbulent eddy and its surroundings so that the effectiveness of the eddy to transport heat was reduced. This effect resulted in lower values of α at low Prandtl numbers. In some of these approaches, average values of α across a pipe were calculated as a function either of Reynolds number and Prandtl number, or the maximum value of ϵ_M/ν_L occurring in the pipe and Prandtl number. In the present study, an expression for the ratio of diffusion coefficients was desired that also included the variation with distance from the wall.

Subbotin, et al[29] reported data obtained for mercury and sodium-potassium alloy. This data indicates that Prandtl number may not have a large effect on the ratio of turbulent diffusion coefficients for liquid metals. However, a trend of increasing α with Reynolds number is indicated at a value of y/r = 0.2. This data is shown in Figure 4. The data of Beckwith and Fahien[20] for water, and of Sesonske, et al[28], Brown, et al[30], and Isakoff and Drew[31] for mercury have been added to this figure. Since this study is aimed primarily at liquid metal heat transfer, data obtained for air was not added to the figure. In general, air results in higher values of α.

Because of the absence of any apparent Prandtl number effect for liquid metals, an equation of the form

$$\alpha = e^{-\frac{a}{(\epsilon_M/\nu_L)^n}}$$
(4a)

was considered. This expression results in values of α varying from zero for ϵ_M / ν_L equal to zero, to 1.0 for ϵ_M / ν_L equal to a very large value. These trends are in agreement with the variation of α near a pipe wall as either distance from the wall or Reynolds number are varied independently. Considering the variation of α with ϵ_M / ν_L at constant Reynolds number, Figures 5 and 6 present the data of Beckwith and Fahien for water and of Sesonske, et al for mercury. It can be seen that at a given Reynolds number, α tends toward zero as the wall is approached. In this region, ϵ_M / ν_L also approaches zero. Therefore, the trend of α approaching zero as ϵ_M / ν_L approaches zero is indicated. The data presented in Figure 4 indicates that at a given y/r, α increases to near one as Reynolds number increases. Since ϵ_M / ν_L at a given y/r increases as Reynolds number increases, the trend of α increasing toward one as ϵ_M / ν_L increases is demonstrated by this data.

The values of the constants a and n were determined using the data of both Sesonske, et al and Beckwith and Fahien for small values of y/r. The constants a and n were found to equal 2.0 and 0.5, respectively. Values of α using the resulting expression are shown plotted in Figures 5 and 6 based on measured values of ϵ_M / ν_L and can be seen to be in poor agreement with most data shown. Calculated values of α were also added to Figure 4. These values were calculated using Deissler's expression for eddy diffusivity variation[22]

$$\frac{\epsilon_M}{\nu_L} = 0.72 \frac{r}{\nu_L} \sqrt{\frac{\tau g_c}{\rho}} (1 - \frac{y}{r})(1 - \sqrt{1 - \frac{y}{r}})$$ (5)

and the expression for friction factor

$$f = \frac{0.184}{Re^{0.2}}$$ (6)

The agreement can be seen to be poor in this figure also.

Although the analytical expression for α does not agree with the data in general, inconsistencies are found in the data which appear to make the determination of an expression that will correlate all available α data very difficult. For example, the data of both Beckwith and

Fahien, and Brown, et al indicate an almost constant value of α for large y/r, but the data of Sesonske, et al, and Isakoff and Drew indicate a decreasing α as y/r increases for values of y/r approaching 1. Also, the data of Brown, et al appears to be much lower than that of other investigators, as indicated in Figure 4.

Although the analytical expression does not result in good general agreement with the considered data, its general trends can be seen to be correct in the region near the wall. This region is most important in its effect on heat transfer coefficients since most of the temperature gradient occurs in this region for conventional fluids. For condensing flow of alkali metals the ratio of eddy diffusion coefficients appears to be unimportant since most of the heat is calculated to be transferred by molecular conduction in the condensate layer when the above expression for α is used. For these reasons the equation which is used in this study for determining α is

$$\alpha = e^{-\frac{2.0}{(\epsilon_M/\nu_L)^{0.5}}} \tag{4b}$$

The variation of α with Reynolds number at y/r = 0.2 was calculated using the present method for the conditions of the data of Beckwith and Fahien. These results are shown in Figure 4 and can be seen to be in good agreement with the results obtained based on Equations (5) and (6).

Equations (1d) and (2d) can now be used to determine the velocity and temperature distributions in terms of the shear stress and heat flux distributions.

From Equation (1d)

$$\frac{du^+}{dy^+} = \frac{\tau}{\tau_0} \frac{1}{\left[1 + \frac{\epsilon_M}{\nu_L}\right]} \tag{7}$$

Substituting Equation (7) into Equation (3)

$$\frac{\epsilon_M}{\nu_L} = K^2 y^{+2} \left[1 - e^{-y^+/A^+}\right]^2 \frac{\tau}{\tau_0} \frac{1}{\left[1 + \frac{\epsilon_M}{\nu_L}\right]}$$

Transposing and rearranging terms

$$\left(\frac{\epsilon_M}{\nu_L}\right)^2 + \frac{\epsilon_M}{\nu_L} - \frac{\tau}{\tau_O} K^2 y^{+2} \left[1 - e^{-y^+/A^+}\right]^2 = 0$$

Solving for $\dfrac{\epsilon_M}{\nu_L}$

$$\frac{\epsilon_M}{\nu_L} = \frac{1}{2}\left[-1 \pm \sqrt{1 + 4\frac{\tau}{\tau_O} K^2 y^{+2}\left[1 - e^{-y^+/A^+}\right]^2}\right] \qquad (8)$$

Since $\dfrac{\epsilon_M}{\nu_L}$ must be zero when $y^+ = 0$, the correct root is the one with the plus sign.

Therefore

$$\frac{\epsilon_M}{\nu_L} = \frac{1}{2}\left[-1 + \sqrt{1 + 4\frac{\tau}{\tau_O} K^2 y^{+2}\left[1 - e^{-y^+/A^+}\right]^2}\right] \qquad (9)$$

Substituting this equation into Equation (7)

$$\frac{du^+}{dy^+} = \frac{\frac{\tau}{\tau_O}}{1 + \frac{1}{2}\left[-1 \sqrt{1 + 4\frac{\tau}{\tau_O} K^2 y^{+2}\left[1 - e^{-y^+/A^+}\right]^2}\right]} \qquad (10)$$

or

$$du^+ = \frac{\frac{\tau}{\tau_O} dy^+}{1 + \frac{1}{2}\left[-1 + \sqrt{1 + 4\frac{\tau}{\tau_O} K^2 y^{+2}\left[1 - e^{-y^+/A^+}\right]^2}\right]} \qquad (11)$$

Integrating from the wall to any radial distance y^+ from the wall

$$u^+ = \int_0^{y^+} \frac{\frac{\tau}{\tau_O} dy^+}{1 + \frac{1}{2}\left[-1 + \sqrt{1 + 4\frac{\tau}{\tau_O} K^2 y^{+2}\left[1 - e^{-y^+/A^+}\right]^2}\right]} \qquad (12)$$

In a similar procedure the following equation for t^+ can be derived.

$$t^+ = \int_0^{y^+} \frac{\frac{q}{q_0} \, dy^+}{\frac{1}{Pr_L} + \frac{\alpha}{2} \left[-1 + \sqrt{1 + 4 \frac{\tau}{\tau_0} K^2 y^{+2} \left[1 - e^{-y^+/A^+}\right]^2} \right]} \quad (13)$$

The following equations for $\frac{\tau}{\tau_0}$ and $\frac{q}{q_0}$ are derived in Appendices A and C using the Navier-Stokes and energy equations

$$\frac{\tau}{\tau_0} = \frac{1 + \frac{r_0}{2\tau_0}\left(-\frac{dp}{d\ell} + \rho_L \frac{g}{g_c} \cos\theta\right)\left(2\left(\frac{y^+}{r_0^+}\right) - \left(\frac{y^+}{r_0^+}\right)^2\right)}{\left(1 - \frac{y^+}{r_0^+}\right)} \quad (14)$$

$$\frac{q}{q_0} = \frac{1}{1 - \frac{y^+}{r_0^+}} \quad (15)$$

The determination of the shear stress distribution from Equation (14) requires knowledge of the wall shear stress τ_0 and the pressure gradient $dP/d\ell$. An expression for the pressure gradient is derived in Appendix B, as follows

$$\frac{dP}{d\ell} = -\left(\frac{dP}{d\ell}\right)_{friction} - \cos\theta \frac{g}{g_c}\left[R_L \rho_L + (1-R_L)\rho_g\right] +$$

$$\frac{2}{\pi g_c}\left(\frac{W_T}{r_0^3}\right)\left(\frac{q_0}{\lambda}\right)\left[2\left(\frac{1-x}{\rho_L R_L} - \frac{x}{\rho_g(1-R_L)}\right) + \left(\frac{(1-x)^2}{\rho_L R_L^2} - \frac{x^2}{\rho_g(1-R_L)^2}\right)\frac{dR_L}{dx}\right] \quad (16)$$

where $\left(\frac{dP}{d\ell}\right)_{friction} = \frac{2 \, \tau_0}{r_0}$ $\quad (16a)$

The determination of the shear stress distribution therefore depends on known or calculated values of local quantities except for $\left(\dfrac{dP}{d\ell}\right)_{friction}$ and $\dfrac{dR_L}{dx}$.

Three different assumptions were made concerning the frictional pressure gradient in order to determine calculated values of condensing coefficients and liquid film thicknesses. The first method of calculation used values of $\left(\dfrac{dP}{d\ell}\right)$ obtained experimentally for a given data point. This enabled $\left(\dfrac{dP}{d\ell}\right)_{friction}$ to be calculated and τ_o determined from Equation (16a). The second method used the correlation derived by Lockhart and Martinelli[32] for adiabatic two-component horizontal two-phase flow to determine $\left(\dfrac{dP}{d\ell}\right)_{friction}$ directly. The third method used the correlation derived by Dukler[33] for adiabatic two-component vertical downflow, to determine the sum of $\left(\dfrac{dP}{d\ell}\right)_{friction}$ and the gravitational pressure gradient which is the second term in the right hand side of Equation (16).

The term $\dfrac{dR_L}{dx}$ is the slope of the variation of liquid fraction with quality at the local point being analyzed. Since the analytical determination of this term would require much more extensive computation, the liquid fraction correlation derived by Lockhart and Martinelli[32] was used to determine the slope. The derivation of the resulting expressions used for this term are presented in Appendix B.

When Equations (14), (15), and (16) are substituted into Equations (12) and (13), all terms under the integral signs become functions of y^+ only, and the two equations can be solved independently.

Equation (12) can be solved to determine u^+ as a function of y^+ by using a numerical integration method such as Simpson's rule or the trapezoidal rule. Once the velocity distribution has been determined, the thickness of the liquid layer can be determined using the known liquid flow rate and the continuity equation derived below.

The differential flow rate through a differential area of flow is

$$dW_L = \rho_L \, u \, dA \tag{17}$$

A differential annular area of flow in a tube is

$$dA = 2\pi \, (r_o - y) \, dy \tag{18}$$

Thus

$$dW_L = 2\pi \, \rho_L \, u \, (r_o - y) \, dy \tag{19}$$

Integrating from the wall to the liquid-vapor interface located at a distance δ from the wall gives the total liquid flow rate.

$$W_L = 2\pi \, \rho_L \int_o^\delta u \, (r_o - y) \, dy \tag{20}$$

Using the definitions of u^+ and y^+ and defining $r_o^+ \equiv \dfrac{r_o \, v^*}{v_L}$, Equation (20) can be rearranged to give

$$W_L = \frac{2\pi \, \rho_L \, v_L^2}{v^*} \int_o^{\delta^+} u^+ (r_o^+ - y^+) \, dy^+ \tag{21}$$

where $\delta^+ = \dfrac{\delta v^*}{v_L}$ and is the nondimensional film thickness.

From Equation (12) u^+ is obtained as a function of y^+ and thus Equation (21) can be integrated numerically. The determination of the liquid film thickness then involves guessing a value of δ^+ until a value is guessed which gives the correct known liquid flow rate. Since the static pressure gradient, $dP/d\ell$ in Equation (14) requires knowledge of film thickness, new values of this term are calculated for each assumed value of δ^+ used in the calculations. The guessing of successive values of δ^+ can be handled by various methods in order to arrive at a final value in a small number of tries.

Once the film thickness is known, Equation (13) can be solved to
obtain the temperature difference from the wall to the edge of the
liquid film $(t_v - t_o)$ and thus the heat transfer coefficient across
the liquid film can be obtained through the following defining equation

$$h_{film} \equiv \frac{q_o}{t_v - t_o} \tag{22}$$

This coefficient h_{film} only involves the temperature difference
due to the thermal resistance of the liquid film. If other thermal
resistances are present at the liquid-vapor interface or at the liquid-
wall interface due to impurities, then an overall coefficient must be
defined. In the case of the liquid-vapor interfacial resistance, an
expression is presented in Reference 13 for the temperature drop at
the liquid-vapor interface in terms of the mass flux

$$m = \left(\frac{\sigma}{2-\sigma}\right)\left(\frac{2}{\pi}\right)^{1/2}\left(\frac{M}{R}\right)^{3/2}\frac{P_{sat}\lambda}{t_v^{5/2}}g_c^{1/2}J(t_v - t_i) \tag{23}$$

In this equation σ is the accommodation or condensation coefficient
which must be determined experimentally.

Since $q = \lambda m$ and $h_{interface} \equiv \frac{q}{t_v - t_i}$

$$h_{interface} = \left(\frac{\sigma}{2-\sigma}\right)\left(\frac{2}{\pi}\right)^{1/2}\left(\frac{M}{R}\right)^{3/2}\frac{P_{sat}\lambda^2}{t_v^{5/2}}g_c^{1/2}J \tag{24}$$

The overall heat transfer coefficient of the tube wall can then be
found including both the liquid film and liquid-vapor interfacial
resistance from

$$\frac{1}{h} = \frac{1}{h_{film}} + \frac{1}{h_{interface}\left(\frac{r_o - \delta}{r_o}\right)} \tag{25}$$

The term ($\frac{r_o - \delta}{r_o}$) accounts for the change in heat flux area from
the wall to the liquid-vapor interface.

V. COMPARISONS WITH DATA

The analytical method presented in the previous section was used to estimate liquid film thicknesses and condensing heat transfer coefficients for a number of conditions for which data was available for comparison. The cases considered were the evaluation of water film thicknesses for air-water mixtures in vertical upflow and vertical downflow and the evaluation of the condensing coefficients for steam in vertical downflow. No horizontal flow cases were analyzed because of the possible large departure from the annular flow pattern in the experimental data. In each of the cases considered, the effect of different methods of predicting wall shear stress was investigated.

Liquid Film Thickness

Vertical Downflow

The analytical method was used for predicting liquid film thickness for comparison with the measured values of Charvonia[34] and Chien[35]. Both of these investigators measured the mean thickness of a water layer flowing along the tube wall when an air-water mixture was flowing in vertical downflow near ambient temperature and pressure. The tube inside diameters were 0.208 ft for Charvonia and 0.167 ft for Chien. Chien found that entrainment of liquid in the gas core occurred above certain values of liquid and gas Reynolds numbers. Since the present analysis does not consider entrainment, no data was used for comparison that indicated entrainment may be present, based upon Chien's criterion for the inception of entrainment. Data points were selected to cover the range of the experimental variables for which no entrainment was expected to be present.

Calculated values of film thickness using measured values of pressure drop are compared with measured values of film thickness obtained by Charvonia and Chien in Figure 7. The agreement can be seen to be good. Figure 8 shows the comparison between the values of film thickness calculated using Dukler's correlation for pressure drop in a vertical pipe and the measured values. Agreement can be seen to be good again. However, when values of film thickness were calculated using Lockhart and

Martinelli's correlation for pressure drop, agreement was found to be poor, as shown in Figure 9. For some cases, this method of obtaining pressure drop resulted in unrealistic calculated velocity profiles in the liquid film so that no solution could be found.

The poor agreement between data and theory using Lockhart and Martinelli's method is probably due to the fact that their correlation is based upon pressure drops measured in horizontal tubes. Dukler's correlation which is based on data from vertical tubes with downflow resulted in good agreement. The agreement between data and theory using measured values of pressure drop indicates the validity of the analysis for predicting film thickness in the range of the data considered.

In order to determine more clearly whether the trends indicated by the theory are correct, Charvonia's film thickness data are plotted in Figures 10 and 11 as a function of vapor and liquid flow rate. Theoretical values are presented which are based upon both measured pressure gradients and pressure gradients calculated using Dukler's method. The agreement can be seen to be good in both cases.

Vertical Upflow

Collier and Hewitt[36] presented mean liquid film thickness data for the upward flow of an air-water mixture in a tube of 0.104 ft inside diameter near ambient temperature and pressure. Liquid film thicknesses were calculated for comparison with this data using the method of Lockhart and Martinelli for estimating pressure gradient. The comparison between theory and values obtained from a mean line through the data is shown in Figure 12. Agreement can be seen to be good. Dukler's method was not used to obtain pressure gradient because of its apparent inapplicability to vertical upflow.

Condensing Heat Transfer Coefficients

Carpenter[37] and Goodykoontz and Dorsch[38] obtained measured values of local condensing heat transfer coefficients for vertical downflow

inside of a tube. Carpenter used water, ethanol, methanol, toluene, and trichloroethylene as the working fluids in a tube of 0.459 inch inside diameter, and Goodykoontz and Dorsch used water in a tube of 0.293 inch inside diameter.

In order to determine the capabilities of the present analysis to predict condensing heat transfer coefficients for flow inside a tube, calculations were made for comparison with data presented in both of the above references. In order to limit the calculations, water was the only working fluid considered from Carpenter's data.

Two adjustments were made to the analytical values to take into account basic effects not initially included. The calculation procedure programmed on the computer includes the assumption that local quality is equal to the ratio of vapor flow to total flow. Therefore, the effect of liquid subcooling in the condensate layer was ignored. Subsequent study of calculated results, indicated that at low qualities this assumption leads to significant error in the calculated values of vapor and liquid flow rates, based on a value of quality determined from a heat balance. Therefore, the temperature and velocity profiles calculated by the analysis were used to determine more accurate values of vapor and liquid flow rates for each case using the equation

$$x = \frac{2\pi \int_0^{r_0} \rho_L u_L i_L \, r dr - W_T i_{L sat}}{W_T (i_{g sat} - i_{L sat})} = \frac{W_g i_{g sat} + 2\pi \int_{r_0-\delta}^{r_0} \rho_L u_L i_L \, r dr - W_T i_{L sat}}{W_T (i_{g sat} - i_{L sat})}$$

(26)

where $i_{g sat}$ and $i_{L sat}$ are the vapor and liquid enthalpies, respectively, evaluated at saturated conditions. The computer program was then rerun using the new flow rates. The importance of this correction for one particular case is indicated in Figure 13 where the percentage difference between W_g/W_T and equilibrium quality based upon local enthalpy is shown as a function of quality based upon enthalpy. No adjustment was found necessary to the analytical values for the experimental conditions of Carpenter because values of flow rates including the effects of subcooling were presented in this reference and were used in the computer program initially.

A second slight adjustment was made to take into account the variation of liquid viscosity across the condensate layer. Results from the initial analysis were used to determine the arithmetic mean film temperature based on wall and saturation temperatures. This mean film temperature was used to calculate a new liquid viscosity and the case rerun. This correction resulted in only a small change in condensing coefficient from the initial value. The importance of this correction is shown in Figure 14 where the calculated condensing coefficient for the conditions of one of Carpenter's data points is plotted as a function of liquid viscosity and temperature at which the viscosity is evaluated.

Calculated values of heat transfer coefficients including these adjustments are compared with measured values in Figures 15 and 16. The calculated values presented in Figures 15 and 16 are based on Lockhart and Martinelli's and Dukler's methods for predicting pressure gradients, respectively. Agreement between data and theory is seen to be good in both cases.

In order to compare the trends of condensing heat transfer coefficient variation with quality as predicted by the theory and obtained experimentally by Goodykoontz and Dorsch and Carpenter, Figures 17 and 18 are shown. The analysis can be seen to be in good agreement with the data over the entire range of experimental data.

The calculated values of condensing heat transfer coefficients for conventional fluids is very dependent on the ratio of eddy diffusion coefficients, α. The fact that agreement between data and theory is obtained indicates that the expression used for α which was obtained for fully-developed single-phase flow may be reasonably accurate in a condensing film.

In order to show the importance of the assumption concerning α, calculations were performed assuming that α equals one. These results are presented in Figures 19 and 20. The assumption of α equalling one can be seen to lead to values of condensing coefficient much higher than those measured experimentally. This result is surprising, considering the success found by previous investigators in correlating data using the assumption that α equals one. Further study of this result is needed.

Figure 21 shows calculated values of velocity and temperature pro-
files across the condensate layer for the conditions of one of Carpenter's
data points, for which the quality was low. The universal velocity pro-
file is plotted for comparison. It is seen that only a small deviation
exists between the two velocity profiles. This result indicates that
liquid film thicknesses and therefore condensing coefficients can be
calculated using the universal velocity profile for this data. In addi-
tion, much of the temperature drop takes place near the wall
($y^+ < 10$). These last two facts enabled previous investigators
to obtain correlations for conventional fluids using the assumptions
that the velocity profile for this data is the universal profile and that
most of the temperature drop occurs in the viscous sublayer. The
distributions of shear stress, turbulent diffusion coefficients of
momentum and heat, and ratio of turbulent diffusion coefficients are
shown in Figure 22 for the same data point. The shear stress can
be seen to decrease rapidly with distance from the wall. This
results in the velocity profile departing slightly from the universal
profile.

The ratio of turbulent diffusion coefficients α can be seen to be
much less than one for the entire film for this case. Also, the ratio
of the turbulent to molecular diffusion coefficients of heat is much
greater than one for the entire turbulent region of the film.

Summary of Data Comparison

The present analysis results in good estimations of liquid film
thickness for annular flow in a vertical tube where no entrainment
is present. Agreement is good for both the downflow data of
Charvonia[34] and Chien[35] and the upflow data of Collier and Hewitt[36].
The best correlation was obtained when the method of Dukler was
used for predicting pressure drop in vertical downflow and the
method of Lockhart and Martinelli for predicting pressure drop in
vertical upflow. Also, the analysis provides calculated values of
local condensing heat transfer coefficients for vertical downflow of
steam which are in good agreement with the data of Carpenter[37] and
Goodykoontz and Dorsch[38], when either Dukler's or Lockhart and
Martinelli's method are used for predicting pressure drop.

VI. THEORETICAL PREDICTION OF CONDENSING HEAT TRANSFER COEFFICIENTS FOR POTASSIUM

Because of the agreement between the present analysis and liquid film thickness and condensing coefficient data of conventional fluids, this analysis may enable the prediction of film thickness and condensing liquid film heat transfer coefficients for liquid metals. These two quantities are simply related for liquid metal condensation since the main mode of heat transfer is by molecular conduction.

In order to demonstrate the values of condensing heat transfer coefficient that can be expected for potassium condensing in downflow inside a tube, calculations were made with quality, flow rate, and accommodation coefficient as independent variables. These are plotted in Figures 23 and 24. In addition, the effects of heat flux rate and of different assumptions concerning frictional pressure gradient were investigated. A basic condition was selected where

$W_{potassium}$ = 40 lbs/hr
$P_{potassium}$ = 6.6 psia
tube inside diameter = 0.625 in.
Q = 60,000 Btu/hr ft^2
No liquid-vapor interfacial resistance
Frictional pressure gradient obtained from Lockhart and
  Martinelli correlation

For these basic conditions, the condensing coefficients were calculated as a function of quality. The flow rate was increased to twice and reduced to one-half the standard flow rate with appropriate adjustments made to the frictional pressure gradient. Then the calculations were repeated. The results for variation of flow rate are presented in Figure 23. The effects of both quality and flow rate can be seen to be very important, as was expected.

The effect of liquid-vapor interfacial resistance on the condensing coefficients at standard conditions is shown in Figure 24. Liquid-vapor interfacial resistances can be seen to be very important, especially at high qualities where the condensing coefficients are high.

Similar calculations were made with the heat flux doubled and halved and everything else at the standard conditions. These results indicated that for the conditions analyzed, heat flux level has essentially no effect on the condensing coefficient.

The importance of the assumed values of frictional pressure gradient is demonstrated in Figure 25 for the standard conditions. Results are shown for values of frictional pressure gradient equal to that obtained from the Lockhart and Martinelli correlation and equal to one-half and twice this value. The effect of pressure gradient can be seen to be important. However, since the Lockhart and Martinelli method led to good agreement for condensing coefficients of conventional fluids, the error introduced by using this method for estimating frictional pressure gradient is not likely to be large. The value at low quality may be somewhat in error since values calculated at a quality of 0.1 using Lockhart and Martinelli's frictional pressure gradient were found to result in unrealistic velocity profiles. A higher frictional pressure gradient would be required to give more realistic profiles.

Calculated velocity and temperature profiles for the case of standard conditions and 50 per cent quality are shown in Figure 26. Again, the velocity profile is very close to the universal velocity profile. From the temperature profile, it can be seen that most of the temperature drop does not occur near the wall ($y^+ < 10$) as is true for conventional fluids. The variation of the temperature is very nearly linear with distance from the wall. The distributions of shear stress, turbulent diffusion coefficients of momentum and heat, and the ratio of the turbulent diffusion coefficients of momentum and heat are plotted in Figure 27. The turbulent diffusion coefficients when plotted separately were put in dimensionless form by dividing each by its respective molecular diffusion coefficient. The turbulent diffusion coefficient of heat is negligible when compared to the molecular value because of the low Prandtl number for potassium. This feature causes the temperature profile to be linear and is much different from results found with water, as indicated in Figure 22.

Since many investigators compare experimental values of condensing coefficient with values determined from Nusselt theory, the theoretical values determined in this study for potassium at the standard

conditions were plotted in terms of the dimensionless groupings used
by Nusselt with accommodation coefficient and quality as independent
variables. These are presented in Figure 28. Seban's turbulent
film results for a Prandtl number of 0.003 are also shown for com-
parison. The results calculated in the present study can be seen to
be much higher than those predicted by the theories of either Nusselt
or Seban when no liquid-vapor interfacial resistance is present.
This result is due primarily to the presence of liquid-vapor inter-
facial shear in the present analysis. A similar effect of interfacial
shear stress was found by Rohsenow, et al[6].

VII. CONCLUSIONS

The following conclusions can be drawn from the results obtained in this report:

A. The present analysis provides an accurate means of predicting liquid film thickness for annular two-component flow of conventional fluids inside tubes with vertical downflow orientation, if the pressure gradient is known. This result indicates the basic validity of the analytical approach.

B. The analysis provides an accurate means of predicting liquid film thickness for annular two-component flow of conventional fluids inside tubes with both vertical upflow and downflow orientations, if the pressure gradient is based on the method of Dukler for downflow and the method of Lockhart and Martinelli for upflow. Therefore the present analysis can be used to predict liquid film thicknesses even when no measured values of pressure gradient are available.

C. The analysis enables the accurate prediction of local condensing heat transfer coefficients for conventional fluids with vertical downflow inside tubes, if the pressure gradient is based on either the method of Dukler or that of Lockhart and Martinelli.

D. Because of the above agreement, the present analysis can be expected to accurately predict the thickness of condensate layers inside condensing tubes for vertical downflow orientation and under zero-gravity conditions.

E. For the cases analyzed, the local values of condensing coefficient for potassium in vertical downflow inside a tube are higher than those calculated using Nusselt's theory for laminar condensing on a vertical surface with no liquid-vapor interfacial shear, if no vapor-liquid interfacial resistance to heat flow is considered.

F. Significant reductions in condensing coefficient for potassium can result from vapor-liquid interfacial resistance for accommodation coefficients as high as 0.9 or greater.

G. The effect of liquid subcooling must be considered when calcu-
    lating condensing vapor and liquid flow rates for a flow of known
    enthalpy and total flow, if the quality of the fluid is low.

H. In many cases the thickness of liquid condensate layers and
    condensing heat transfer coefficients may be calculated using
    the universal velocity profile because of the small departure of
    the calculated velocity profiles from the universal velocity
    profile.

I. Condensing heat transfer coefficients calculated assuming that
    the ratio of turbulent diffusion coefficients of heat and momentum
    equals one may be in significant error.

APPENDIX A

Derivation of Shear Stress Distribution Equation

APPENDIX A

Derivation of Shear Stress Distribution Equation

The Navier-Stokes equation (See Reference 39) for laminar incompressible flow in the axial direction written in cylindrical coordinates is

$$\rho_L \left(\frac{\partial u}{\partial t} + v \frac{\partial u}{\partial r} + \frac{w}{r} \frac{\partial u}{\partial \phi} + u \frac{\partial u}{\partial z} \right) =$$

$$F - \frac{\partial P}{\partial z} + \mu_L \left(\frac{\partial^2 u}{\partial r^2} + \frac{1}{r} \frac{\partial u}{\partial r} + \frac{1}{r^2} \frac{\partial^2 u}{\partial \phi^2} + \frac{\partial^2 u}{\partial z^2} \right) \qquad (A1)$$

Where:

   v = velocity component in outward radial direction (r direction)
   u = velocity component in axial direction (z direction)
   w = velocity component in tangential direction (ϕ direction)
   F = the body force in z direction
   $\frac{\partial P}{\partial z}$ = static pressure gradient in z direction

Although this equation holds for laminar flow, it is assumed that turbulent flow can be treated using this equation when turbulent diffusion coefficients are added to the molecular terms.

Since the flow is steady $\frac{\partial u}{\partial t} = 0$ and since the flow is axisymmetric $\frac{\partial u}{\partial \phi} = 0$ and $\frac{\partial^2 u}{\partial \phi^2} = 0$

Thus the equation becomes

$$\rho_L v \frac{\partial u}{\partial r} + \rho_L u \frac{\partial u}{\partial z} = F - \frac{\partial P}{\partial z} + \mu_L \left(\frac{\partial^2 u}{\partial r^2} + \frac{1}{r} \frac{\partial u}{\partial r} + \frac{\partial^2 u}{\partial z^2} \right)$$
$$(A2)$$

Of the terms $\frac{\partial^2 u}{\partial r^2}$, $\frac{1}{r} \frac{\partial u}{\partial r}$, and $\frac{\partial^2 u}{\partial z^2}$, the latter term is very small compared to the first two terms since changes of the axial velocity in the axial direction occur at a much smaller rate than changes of the axial velocity component in the radial direction; for example, the ratio of $\frac{\partial^2 u}{\partial r^2}$ to $\frac{\partial^2 u}{\partial z^2}$ is in the order of the square of the tube length to film thickness ratio which is a very large number. Therefore, the $\frac{\partial^2 u}{\partial z^2}$ term can be neglected, and

$$\rho_L \left(v \frac{\partial u}{\partial r} + u \frac{\partial u}{\partial z} \right) = F - \frac{\partial P}{\partial z} + \mu_L \left(\frac{\partial^2 u}{\partial r^2} + \frac{1}{r} \frac{\partial u}{\partial r} \right) \tag{A3}$$

The shear stress component in the r plane and z direction is

$$\tau = -\mu_L \left(\frac{\partial v}{\partial z} + \frac{\partial u}{\partial r} \right) \tag{A4}$$

Since $\frac{\partial v}{\partial z} \ll \frac{\partial u}{\partial r}$,

$$\tau = -\mu_L \frac{\partial u}{\partial r} \tag{A5}$$

and

$$r\tau = -r \mu_L \frac{\partial u}{\partial r} \tag{A6}$$

Taking the partial derivative of Equation (A6) with respect to r

$$\frac{\partial (r \tau)}{\partial r} = -\mu_L \left(r \frac{\partial^2 u}{\partial r^2} + \frac{\partial u}{\partial r} \right) \tag{A7}$$
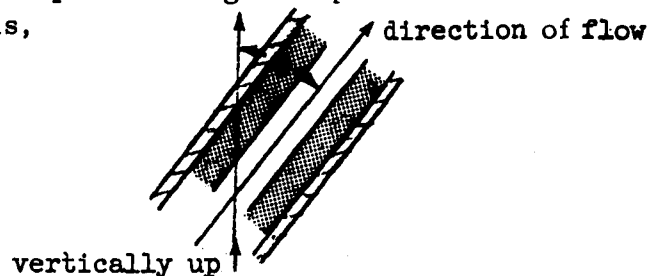
Dividing by r and rearranging

$$\frac{1}{r} \frac{\partial (r \tau)}{\partial r} = -\mu_L \left(\frac{\partial^2 u}{\partial r^2} + \frac{1}{r} \frac{\partial u}{\partial r} \right) \tag{A8}$$

Substituting Equation (A8) into Equation (A3)

$$\rho_L v \frac{\partial u}{\partial r} + \rho_L u \frac{\partial u}{\partial z} = F - \frac{\partial P}{\partial z} - \frac{1}{r} \frac{\partial (r \tau)}{\partial r} \tag{A9}$$

The body force term F consists of the gravitational force per unit volume on the liquid. Using the upward vertical direction as the reference axis,

the gravitational force on the liquid is $-\rho_L \dfrac{g}{g_c} \cos \theta$, where θ is the angle measured from the vertical upward direction.

Thus
$$F = -\rho_L \frac{g}{g_c} \cos \theta \qquad\qquad (A10)$$

Substituting Equation (A10) into Equation (A9)

$$\rho_L v \frac{\partial u}{\partial r} + \rho_L u \frac{\partial u}{\partial z} = -\rho_L \frac{g}{g_c} \cos \theta - \frac{\partial P}{\partial z} - \frac{1}{r} \frac{\partial (r \tau)}{\partial r} \quad (A11)$$

The terms on the left hand side of Equation (A11) are neglected in many boundary layer and condensing flow analyses[5, 6, 7, 10], since these terms greatly increase the complexity of any analytic solution and little error was found to be introduced. These terms are both equal to zero for fully-developed flow since for that case v and $\partial u/\partial z$ are both zero. These terms may not be negligible for the case of condensing flow and must be evaluated from the results of the calculations to see if they can truly be neglected. Such a test is still not a positive proof of the error involved in neglecting these terms.

Neglecting these terms, the Navier-Stokes equation becomes

$$-\rho_L \frac{g}{g_c} \cos \theta - \frac{\partial P}{\partial z} - \frac{1}{r} \frac{\partial (r \tau)}{\partial r} = 0 \qquad (A12)$$

or

$$-\frac{1}{r} \frac{\partial (r \tau)}{\partial r} = \rho_L \frac{g}{g_c} \cos \theta + \frac{\partial P}{\partial z} \qquad (A13)$$

The term $\dfrac{\partial P}{\partial z}$ is the local static pressure gradient (i.e. the one which could be measured with static taps) and thus will be written in the more familar fashion as $dP/d\ell$.

Thus

$$- \frac{1}{r} \frac{\partial (r \tau)}{\partial r} = \rho_L \frac{g}{g_c} \cos \theta + \frac{dP}{d\ell} \qquad (A14)$$

Multiplying both sides by $r \, \partial r$

$$- \partial (r\tau) = \left(\rho_L \frac{g}{g_c} \cos \theta + \frac{dP}{d\ell} \right) r \, \partial r \qquad (A15)$$

Integrating

$$- r \tau = \left(\rho_L \frac{g}{g_c} \cos \theta + \frac{dP}{d\ell} \right) \frac{r^2}{2} + C_1 \qquad (A16)$$

At $r = r_o$, $\tau = \tau_o$

Thus

$$- r_o \tau_o = \left(\rho_L \frac{g}{g_c} \cos \theta + \frac{dP}{d\ell} \right) \frac{r_o^2}{2} + C_1 \qquad (A17)$$

Solving for C_1

$$C_1 = - r_o \tau_o - \left(\rho_L \frac{g}{g_c} \cos \theta + \frac{dP}{d\ell} \right) \frac{r_o^2}{2} \qquad (A18)$$

Substituting Equation (A18) into Equation (A16)

$$- r \tau = \left(\rho_L \frac{g}{g_c} \cos \theta + \frac{dP}{d\ell} \right) \frac{r^2 - r_o^2}{2} - r_o \tau_o \qquad (A19)$$

Multiplying both sides by $\frac{-1}{r \tau_o}$

$$\frac{\tau}{\tau_o} = \frac{-1}{r} \left[\left(\rho_L \frac{g}{g_c} \cos \theta + \frac{dP}{d\ell} \right) \frac{r^2 - r_o^2}{2 \tau_o} - r_o \right] \qquad (A20)$$

Noting that $\quad r = r_o - y \quad$ where y is the distance from the wall radially inward

$$\frac{\tau}{\tau_o} = \frac{-1}{r_o - y} \left[\left(\rho_L \frac{g}{g_c} \cos\theta + \frac{dP}{d\ell} \right) \frac{(r_o - y)^2 - r_o^2}{2\,\tau_o} - r_o \right] \quad (A21)$$

or

$$\frac{\tau}{\tau_o} = \frac{-1}{r_o - y} \left[\left(\rho_L \frac{g}{g_c} \cos\theta + \frac{dP}{d\ell} \right) \frac{r_o^2 - 2yr_o + y^2 - r_o^2}{2\,\tau_o} - r_o \right] \quad (A22)$$

Cancelling equal terms of opposite sign and factoring out r_o from the right side gives

$$\frac{\tau}{\tau_o} = \frac{-r_o}{r_o - y} \left[\left(\rho_L \frac{g}{g_c} \cos\theta + \frac{dP}{d\ell} \right) \frac{(y^2/r_o) - 2y}{2\,\tau_o} - 1 \right] \quad (A23)$$

or

$$\frac{\tau}{\tau_o} = \frac{1 - \dfrac{r_o}{2\tau_o} \left(\rho_L \dfrac{g}{g_c} \cos\theta + \dfrac{dP}{d\ell} \right) \left(\dfrac{y^2}{r_o^2} - \dfrac{2y}{r_o} \right)}{1 - \dfrac{y}{r_o}} \quad (A24)$$

Since $\quad \dfrac{y}{r_o} = \dfrac{y+}{r_o +} \quad$ the final shear stress equation is

$$\frac{\tau}{\tau_o} = \frac{1 + \dfrac{r_o}{2\tau_o} \left(\rho_L \dfrac{g}{g_c} \cos\theta + \dfrac{dP}{d\ell} \right) \left(2 \left(\dfrac{y+}{r_o +} \right) - \left(\dfrac{y+}{r_o +} \right)^2 \right)}{1 - \dfrac{y+}{r_o +}} \quad (A25)$$
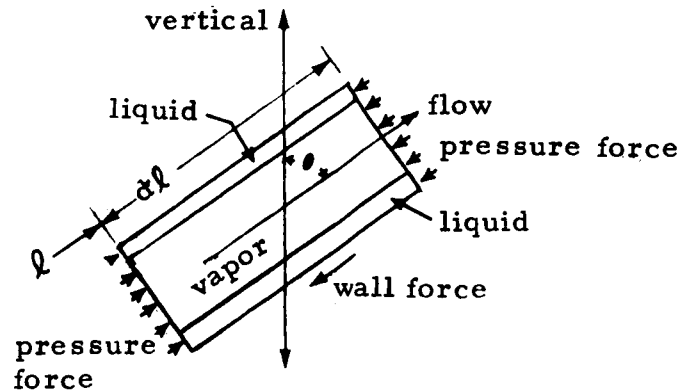
APPENDIX B

Derivation of Pressure Gradient Equation

APPENDIX B

Derivation of Pressure Gradient Equation

The static pressure gradient $\dfrac{dP}{d\ell}$ is obtainable from the momentum

equation written for the entire two-phase stream. The static pressure is assumed to be uniform across the tube.

Consider the differential element along the length of the tube.

The momentum equation is

$$\sum \text{forces} = \text{change in momentum flux}$$

or

wall force + pressure force + gravitational force = change in momentum flux

The wall force is $\quad - \tau_0 \left(2\pi r_0 \right) d\ell$

Since for adiabatic flow without gravitational forces

$$\tau_0 = \frac{r_0}{2} \left(\frac{dP}{d\ell} \right)_{\text{friction}}$$

the wall force is

$$- \pi r_0^2 \left(\frac{dP}{d\ell} \right)_{\text{friction}} d\ell \tag{B1}$$

Here $(\frac{dP}{d\ell})_{friction}$ is defined as a postive quantity.

The pressure force term is

$$- \pi r_0^2 \, dP = - \pi r_0^2 \, \frac{dP}{d\ell} \, d\ell \qquad\qquad (B2)$$

The gravitational force term is equal to the axial component of the weight of the fluid in the differential length; that is

$$- \pi r_0^2 \cos\theta \, \frac{g}{g_c} \left(R_L \, \rho_L + (1 - R_L) \, \rho_g \right) d\ell \qquad\qquad (B3)$$

where R_L is the fraction of the differential volume that is liquid. The change in momentum flux across the differential element is approximately

$$\left(R_L A \, \frac{\rho_L V_L^2}{g_c} + (1 - R_L) \frac{A \rho_g V_g^2}{g_c} \right) - \left(\frac{R_L A \rho_L V_L^2}{g_c} + \frac{A(1 - R_L) \rho_g V_g^2}{g_c} \right)$$

$$\text{at Station } \ell + d\ell \qquad\qquad\qquad \text{at Station } \ell$$

$$(B4)$$

where V_L and V_g are flow average velocities defined by the continuity equations, $W_L = \rho_L V_L A R_L$ and $Wg = \rho g Vg A (1 - R_L)$

Therefore,

$$V_L^2 = \left(\frac{W_L}{\rho_L A R_L} \right)^2 \qquad\qquad (B5)$$

and

$$Vg^2 = \left(\frac{Wg}{\rho g A (1 - R_L)} \right)^2 \qquad\qquad (B6)$$

Substituting Equations (B5) and (B6) into (B4)

$$\Delta\text{ momentum flux} = \left(\frac{W_L^2}{\rho_L A R_L g_c} + \frac{W_g^2}{\rho_g A(1-R_L)g_c} \right)_{\text{at Station } \ell + d\ell}$$

$$- \left(\frac{W_L^2}{\rho_L A R_L g_c} + \frac{W_g^2}{\rho_g A(1-R_L)g_c} \right)_{\text{at Station } \ell} \qquad (B7)$$

which can be written in differential form as

$$d(\text{momentum flux}) = d \left(\frac{W_L^2}{\rho_L A R_L g_c} + \frac{W_g^2}{\rho_g A(1-R_L) g_c} \right) \qquad (B8)$$

The tube area A is constant with length and the density for condensing flow is considered independent of length. Thus

$$d(\text{momentum flux}) = \frac{1}{\rho_L A g_c} d\left(\frac{W_L^2}{R_L} \right) + \frac{1}{\rho_g A g_c} d\left(\frac{W_g^2}{(1-R_L)} \right) \qquad (B9)$$

or

$$d(\text{momentum flux}) = \frac{1}{\pi r_0^2 g_c} \left[\frac{1}{\rho_L} d\left(\frac{W_L^2}{R_L} \right) + \frac{1}{\rho_g} d\left(\frac{W_g^2}{1-R_L} \right) \right] \qquad (B10)$$

The differentials on the right side can be expanded to give

$$d\left(\frac{W_L^2}{R_L} \right) = \frac{2 W_L \, dW_L}{R_L} - \frac{W_L^2}{R_L^2} \, dR_L \qquad (B11)$$

and

$$d\left(\frac{W_g^2}{1-R_L} \right) = \frac{2 W_g \, dW_g}{(1-R_L)} + \frac{W_g^2}{(1-R_L)^2} \, dR_L \qquad (B12)$$

Since $W_g = x W_T$, then $dW_g = W_T\, dx$ $\qquad$ (B13)

and since $W_L = (1-x)\, W_T$, then $dW_L = -W_T\, dx$ $\qquad$ (B14)

Incorporating Equations (B13) and (B14) into Equations (B11) and (B12),

$$d\left(\frac{W_L^2}{R_L}\right) = \frac{-2(1-x)\, W_T^2}{R_L}\, dx - \frac{(1-x)^2\, W_T^2}{R_L^2}\, dR_L \qquad \text{(B15)}$$

$$d\left(\frac{W_g^2}{1-R_L}\right) = \frac{2x W_T^2}{1-R_L}\, dx + \frac{x^2\, W_T^2}{(1-R_L)^2}\, dR_L \qquad \text{(B16)}$$

Incorporating Equations (B15) and (B16) into Equation (B10),

$$d\,(\text{momentum flux}) = \frac{1}{\pi r_0^2 g_c}\left(\frac{-2(1-x)W_T^2}{\rho_L R_L}\, dx - \frac{(1-x)^2\, W_T^2}{\rho_L R_L^2}\, dR_L \right.$$

$$\left. + \frac{2x W_T^2}{\rho_g(1-R_L)}\, dx + \frac{x^2\, W_T^2}{\rho_g(1-R_L)^2}\, dR_L \right) \qquad \text{(B17)}$$

Factoring out W_T^2 and rearranging terms,

$$d(\text{momentum flux}) = \frac{-1}{\pi g_c}\left(\frac{W_T}{r_0}\right)^2 \left[2\left(\frac{1-x}{\rho_L R_L} - \frac{x}{\rho_g(1-R_L)} \right) dx \right.$$

$$\left. + \left(\frac{(1-x)^2}{\rho_L R_L^2} - \frac{x^2}{\rho_g(1-R_L)^2}\right) dR_L \right] \qquad \text{(B18)}$$

Since R_L is a function of W_T, fluid properties, and x in the correlation of Lockhart and Martinelli[32], $dR_L = \frac{(dR_L)}{dx} \, dx$ for this case.

Therefore,

$$d(\text{momentum flux}) = \frac{-1}{\pi g_c}\left(\frac{W_T}{r_0}\right)^2 \left[2\left(\frac{(1-x)}{\rho_L R_L} - \frac{x}{\rho_g(1-R_L)}\right) \right.$$

$$\left. + \left(\frac{(1-x)^2}{\rho_L R_L^2} - \frac{x^2}{\rho_g(1-R_L)^2}\right)\frac{dR_L}{dx} \right] dx \quad (B19)$$

and

$$d(\text{momentum flux}) = \frac{-1}{\pi g_c}\left(\frac{W_T}{r_0}\right)^2 \left[2\left(\frac{(1-x)}{\rho_L R_L} - \frac{x}{\rho_g(1-R_L)}\right) \right.$$

$$\left. + \left(\frac{(1-x)^2}{\rho_L R_L^2} - \frac{x^2}{\rho_g(1-R_L)^2}\right)\frac{dR_L}{dx} \right]\frac{dx}{d\ell}\, d\ell \quad (B20)$$

The local heat flux into the tube $q_0 = W_T \; \lambda \; \frac{dx}{dA}$ $\qquad$ (B21)

where $\quad dA = 2\pi r_0 \, d\ell \quad$ and sensible heat has been neglected.

Thus
$$q_0 = \frac{W_T \lambda}{2\pi r_0}\;\frac{dx}{d\ell} \qquad\qquad (B22)$$

and
$$\frac{dx}{d\ell} = \frac{2\pi r_0 q_0}{W_T \lambda} \qquad\qquad (B23)$$

Substituting this expression for $\frac{dx}{d\ell}$ into Equation (B20), it becomes

$$d(\text{momentum flux}) = \frac{-2}{g_c}\left(\frac{W_T}{r_0}\right)\left(\frac{q_0}{\lambda}\right)\left[2\left(\frac{1-x}{\rho_L R_L} - \frac{x}{\rho_g(1-R_L)}\right) \right.$$

$$\left. + \left(\frac{(1-x)^2}{\rho_L R_L^2} - \frac{x^2}{\rho_g(1-R_L)^2}\right)\frac{dR_L}{dx} \right] d\ell \quad (B24)$$

All terms in this equation can be evaluated from known local quantities except for $\frac{dR_L}{dx}$. In order to transform the $\frac{dR_L}{dx}$ term into known local quantities requires use of an empirical method or a more complex iterative procedure for solution. An empirical expression was used in this program. The derivation of this expression for $\frac{dR_L}{dx}$ in terms of known quantities will be presented later. $\frac{dR_L}{dx}$ is a function of ρ_g, ρ_L, μ_L, μ_g, x, r_0, and W_T.

The term R_L is the fraction of the tube area at ℓ which contains liquid. Thus, it is related to the thickness of the condensate film through the equation

$$R_L = 1 - \left(1 - \frac{\delta}{r_0}\right)^2 \tag{B25}$$

or

$$R_L = 1 - \left(1 - \frac{\delta+}{r_0^+}\right)^2 \tag{B26}$$

Substituting the expressions from Equations (B1), (B2), (B3), and (B24) into the momentum equation for the entire fluid stream,

$$-\pi r_0^2 \left(\frac{dP}{d\ell}\right)_{friction} d\ell - \pi r_0^2 \frac{dP}{d\ell} d\ell - \pi r_0^2 \cos\theta \frac{g}{g_c}\left(R_L \rho_L\right.$$

$$+ (1-R_L)\rho_g\bigg) = \frac{-2}{g_c}\left(\frac{W_T}{r_0}\right)\left(\frac{q_0}{\lambda}\right)\left[2\left(\frac{1-x}{\rho_L R_L} - \frac{x}{\rho_g(1-R_L)}\right)\right.$$

$$+ \left(\frac{(1-x)^2}{\rho_L R_L^2} - \frac{x^2}{\rho_g(1-R_L)^2}\right)\frac{dR_L}{dx}\bigg] d\ell \tag{B27}$$

Dividing through by $-\pi r_0^2 d\ell$

$$\left(\frac{dP}{d\ell}\right)_{friction} + \frac{dP}{d\ell} + \cos\theta \frac{g}{g_c}\left(R_L \rho_L + (1-R_L)\rho_g\right)$$

$$= \frac{2}{\pi g_c}\left(\frac{W_T}{r_0^3}\right)\left(\frac{q_0}{\lambda}\right)\left[2\left(\frac{1-x}{\rho_L R_L} - \frac{x}{\rho_g(1-R_L)}\right)\right.$$

$$+ \left(\frac{(1-x)^2}{\rho_L R_L^2} - \frac{x^2}{\rho_g(1-R_L)^2}\right)\frac{dR_L}{dx}\bigg] \tag{B28}$$

Solving for $\frac{dP}{d\ell}$

$$\frac{dP}{d\ell} = -\left(\frac{dP}{d\ell}\right)_{friction} - \cos\theta \frac{g}{g_c}\left(R_L \rho_L + (1-R_L)\rho_g\right)$$

$$+ \frac{2}{\pi g_c}\left(\frac{W_T}{r_0^3}\right)\left(\frac{q_0}{\lambda}\right)\left[2\left(\frac{1-x}{\rho_L R_L} - \frac{x}{\rho_g(1-R_L)}\right)\right.$$

$$+ \left(\frac{(1-x)^2}{\rho_L R_L^2} - \frac{x^2}{\rho_g(1-R_L)^2}\right)\frac{dR_L}{dx}\bigg] \tag{B29}$$

This expression for $dP/d\ell$, together with empirical relationships for $(dP/d\ell)_{friction}$ and dR_L/dx can be substituted into Equation (A25) to give the shear stress distribution across the liquid film.

In order to determine the rate of change of liquid fraction R_L with quality x using only local quantities at a given axial station in the case being analyzed, the empirical method of Lockhart and Martinelli[32] was used. They found that R_L could be correlated as a function of X, which is the square root of the ratio of the vapor to liquid pressure drops if these phases were flowing alone in the entire pipe. This enables dR_L/dx to be found since

$$\frac{dR_L}{dx} = \frac{dR_L}{dX} \quad \frac{dX}{dx} \tag{B30}$$

Lockhart and Martinelli's correlating line of R_L versus X was fitted with the following equation

$$R_L = \frac{0.299 \, X^{0.756}}{0.299 \, X^{0.756} + 1} \tag{B31}$$

Using this equation dR_L/dX can be found by differentiation

$$\frac{dR_L}{dX} = \frac{0.226}{X^{0.244}(1.0 + 0.299X^{0.756})^2} \tag{B32}$$

The expressions for X to be used in this equation depend upon the flow regimes, laminar or turbulent, in both the vapor and liquid streams[32]

laminar liquid-laminar vapor

$$Xvv = \left(\frac{\rho_g}{\rho_L} \quad \frac{\mu_L}{\mu_g} \right)^{0.5} \left(\frac{1-x}{x} \right)^{0.5} \tag{B33}$$

turbulent liquid-turbulent vapor

$$X_{tt} = \left(\frac{\rho_g}{\rho_L}\right)^{0.5} \left(\frac{\mu_L}{\mu_g}\right)^{0.1} \left(\frac{1-x}{x}\right)^{0.9} \tag{B34}$$

turbulent liquid-laminar vapor

$$X_{tv} = Re_L{}^{0.4} \left(\frac{0.046}{16}\right)^{0.5} \left(\frac{\rho_g}{\rho_L} \frac{\mu_L}{\mu_g}\right)^{0.5} \left(\frac{1-x}{x}\right)^{0.5} \tag{B35}$$

laminar liquid-turbulent vapor

$$X_{vt} = \left(\frac{16}{0.046}\right)^{0.5} \frac{1}{Re_g{}^{0.4}} \left(\frac{\rho_g}{\rho_L} \frac{\mu_L}{\mu_g}\right)^{0.5} \left(\frac{1-x}{x}\right)^{0.5} \tag{B36}$$

Transition is considered to occur when the Reynolds number of either fluid, calculated assuming it completely fills the pipe radius, is 1000. From these equations for X, the four expressions for $\frac{dX}{dx}$ can be found by differentiation

$$\frac{dX_{vv}}{dx} = -0.5 \left(\frac{\rho_g}{\rho_L} \frac{\mu_L}{\mu_g}\right)^{0.5} \left(\frac{x}{1-x}\right)^{0.5} \left(\frac{1}{x^2}\right) \tag{B37}$$

$$\frac{dX_{tt}}{dx} = \frac{-0.9}{x^2} \left(\frac{\rho_g}{\rho_L}\right)^{0.5} \left(\frac{\mu_L}{\mu_g}\right)^{0.1} \left(\frac{x}{1-x}\right)^{0.1} \tag{B38}$$

$$\frac{dX_{tv}}{dx} = \frac{-Re_L{}^{0.4}}{18.65} \left(\frac{\rho_g}{\rho_L} \frac{\mu_L}{\mu_g}\right)^{0.5} \left(\frac{0.4x+0.5}{x^{1.5}(1-x)^{0.5}}\right) \tag{B39}$$

$$\frac{dX_{vt}}{dx} = \frac{-18.65}{Re_g{}^{0.4}} \left(\frac{\rho_g}{\rho_L} \frac{\mu_L}{\mu_g}\right)^{0.5} \left(\frac{0.9-0.4x}{x^{1.5}(1-x)^{0.5}}\right) \tag{B40}$$

where the Reynolds numbers are the full bore Reynolds numbers mentioned above.

Combining Equations (B30) and (B32) with Equations (B37) through (B40), the expressions for $\frac{dR_L}{dx}$ are obtained for the four flow regimes.

$$\left.\frac{dR_L}{dx}\right|_{vv} = \frac{-0.113}{X_{vv}^{0.244}(1.0+0.299X_{vv}^{0.756})^2}\left(\frac{\rho_g}{\rho_L}\frac{\mu_L}{\mu_g}\right)^{0.5}\left(\frac{x}{1-x}\right)^{0.5}\left(\frac{1}{x^2}\right)$$

$$(B41)$$

where X_{vv} can be obtained from Equation (B33)

$$\left.\frac{dR_L}{dx}\right|_{tt} = \frac{-0.204}{X_{tt}^{0.244}(1.0+0.299\,X_{tt}^{0.756})^2\,x^2}\left(\frac{\rho_g}{\rho_L}\right)^{0.5}\left(\frac{\mu_L}{\mu_g}\right)^{0.1}\left(\frac{x}{1-x}\right)^{0.1}$$

$$(B42)$$

where X_{tt} can be obtained from Equation (B34)

$$\left.\frac{dR_L}{dx}\right|_{tv} = \frac{-0.0121\,Re_L^{0.4}}{X_{tv}^{0.244}(1.0+0.299\,X_{tv}^{0.756})^2}\left(\frac{\rho_g}{\rho_L}\frac{\mu_L}{\mu_g}\right)^{0.5}\left(\frac{0.4x+0.5}{x^{1.5}(1-x)^{0.5}}\right)$$

$$(B43)$$

where X_{tv} can be obtained from Equation (B35)

$$\left.\frac{dR_L}{dx}\right|_{vt} = \frac{-4.21}{X_{vt}^{0.244}(1.0+0.299\,X_{vt}^{0.756})^2\,Re_g^{0.4}}\left(\frac{\rho_g}{\rho_L}\frac{\mu_L}{\mu_g}\right)^{0.5}\left(\frac{0.9-0.4x}{x^{1.5}(1-x)^{0.5}}\right)$$

$$(B44)$$

where X_{vt} can be obtained from Equation (B36). Equations (B41) through (B44), together with Equations (B33) through (B35), enable dR_L/dx to be determined as a function of known local quantities.

APPENDIX C

Derivation of Heat Flux Distribution Equation

APPENDIX C

Derivation of Heat Flux Distribution Equation

The derivation of the heat flux distribution equation depends upon the assumption that the amount of heat convection in the liquid film and conduction in the axial direction are negligible compared to the total heat transferred in the radial direction (see sketch below)
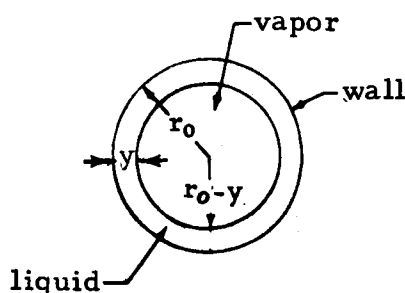
The heat transferred at the wall and at any distance y from wall in the liquid film are equal; thus $Q_0 = Q_y$

The area at the wall for a unit length is $A_0 = 2\pi r_0$

The area at the location y from the wall is $A_y = 2\pi (r_0 - y)$

Since $\quad q_0 = \dfrac{Q_0}{A_0} \quad$ and $\quad q = \dfrac{Q_y}{A_y}$

$$q_0 = \frac{Q_0}{2\pi r_0} \quad \text{and} \quad q = \frac{Q_y}{2\pi (r_0 - y)} = \frac{Q_0}{2\pi(r_0 - y)}$$

Thus

$$\frac{q}{q_0} = \frac{2\pi (r_0)\; Q_0}{2\pi (r_0 - y)\; Q_0} = \frac{r_0}{r_0 - y} = \frac{1}{1 - \dfrac{y}{r_0}}$$

Since

$$\frac{y}{r_0} = \frac{y^+}{r_0^+} \quad , \qquad \frac{q}{q_0} = \frac{1}{1 - \dfrac{y^+}{r_0^+}} \qquad\qquad (C1)$$

APPENDIX D

Nomenclature

NOMENCLATURE

A^+	van Driest turbulent damping constant
C_{Pg}	specific heat of vapor at constant pressure, Btu/lb$_m$ °R
C_{P_L}	specific heat of liquid at constant pressure, Btu/lb$_m$ °R
g	acceleration of gravity, ft/hr^2
g_c	gravitational constant, lb$_m$ ft/lb$_f$ hr^2
h	local heat transfer coefficient, Btu/hr sq ft °R
h_{film}	local heat transfer coefficient of liquid film, Btu/hr sq ft °R
$h_{interface}$	local heat transfer coefficient of interfacial resistance, Btu/hr sq ft °R
i	enthalpy, Btu/lb$_m$
J	mechanical equivalent of heat, ft lb$_f$/Btu
K	Prandtl mixing length constant
k_L	liquid thermal conductivity, Btu/ft hr °R
ℓ	axial length, ft
m	rate of condensation per unit area lb$_m$/hr ft^2
M	molecular weight of vapor, lb$_m$/lb$_m$ mole
P	local static pressure, lb$_f$/sq ft
P_{sat}	vapor pressure, lb$_f$/sq ft
Pr_L	Prandtl number of liquid
q	heat flux at any position y, Btu/hr sq ft
q_o	heat flux at the wall, Btu/hr sq ft
R	universal gas constant, ft lb$_f$/lb$_m$ mole °R
R_L	liquid fraction
r	radial distance from tube axis, ft
r_o	pipe radius, ft
r_o^+	dimensionless pipe radius defined on page 16
t	local temperature at position y, °R
t_i	liquid temperature at liquid-vapor interface, °R
t_o	temperature at the wall, °R
t_v	saturation temperature, °R
t^+	dimensionless temperature defined on page 8
u	local velocity at position y, ft/hr
u^+	dimensionless velocity defined on page 8
V_L	average liquid velocity, ft/hr
V_g	average vapor velocity, ft/hr
v^*	friction velocity $= \sqrt{\dfrac{\tau_o \, g_c}{\rho_L}}$, ft/hr
W_g	gas flow rate, lb$_m$/hr
W_L	liquid flow rate, lb$_m$/hr
W_T	total flow rate, lb$_m$/hr
x	quality, W_g/W_T
y	distance from wall, ft
y^+	dimensionless distance defined on page 8
$\dfrac{dP}{d\ell}$	static pressure gradient, lb$_f$/cu ft

a	ratio of eddy diffusivities
ϵ_H	eddy diffusivity for heat, sq ft/hr
ϵ_M	eddy diffusivity for momentum, sq ft/hr
δ	thickness of liquid film, ft
δ^+	dimensionless thickness of liquid film
θ	angle of pipe orientation measured from vertical upward, degrees
λ	latent heat of vaporization, Btu/lb_m
μ_g	vapor dynamic viscosity, $lb_m/ft\ hr$
μ_{L}	liquid dynamic viscosity, $lb_m/ft\ hr$
ν_L	liquid kinematic viscosity, sq ft/hr
ρ_g	gas density, $lb_m/cu\ ft$
ρ_L	liquid density, $lb_m/cu\ ft$
σ	accommodation coefficient
τ	shear stress, $lb_f/sq\ ft$
τ_0	shear stress at wall, $lb_f/sq\ ft$

APPENDIX E

References

APPENDIX E

References

1. Hess, H. L., H. R. Kunz and S. S. Wyde, Analytical Study of Liquid Metal Condensers, Vol. 1, Design Study PWA Report 2320, NASA Report CR 54224, July 1964

2. Colburn, A. P., Trans. AIChE 30, 187, 1933

3. Carpenter, E. F., and A. P. Colburn, Proc. General Disc. Heat Transfer, Inst. of Mech. Engr. and ASME, pp. 20-26, July 1951

4. Bergelin, O. P., P. K. Kegel, F. G. Carpenter and Carl Gazley, Jr., Co-Current Gas-Liquid Flow II. Flow in Vertical Tubes, Heat Transfer and Fluid Mechanics Institute, Published ASME, 1949

5. Seban, R. A., Trans. ASME, 76, 299, Feb. 1954

6. Rohsenow, W. M., T. H. Weber and A. T. Ling, Trans. ASME 78, 1637-43, 1956

7. Altman, M., F. W. Staub and R. H. Norris, Chem. Eng. Progr., Symp. Vol. 56, No. 36, p. 151, 1960

8. Martinelli, R. C., Trans. ASME, Vol. 69, No. 8, pp. 947-959, Nov. 1947

9. Martinelli, R. C., and D. D. Nelson, Prediction of Pressure Drop During Forced Circulation Boiling of Water, Trans. ASME, Vol. 70, 1948

10a. Dukler, A. E., Chem. Eng. Prog. Symp. Series Vol. 56, No. 30 pp. 1-10, 1960

10b. Dukler, A. E., Appendix to 10a Document 6058, American Documentation Inst., Photoduplication Service, Library of Congress, Washington, D. C.

11. Deissler, R.G., Heat Transfer and Fluid Friction for Fully-Developed Turbulent Flow of Air and Supercritical Water with Variable Fluid Properties, Trans ASME Vol. 76, No. 1, 1954, p. 73

12. Kirillov, P.L., V.I. Subbotin, M.Ya. Suvorov and M.F. Troyanov, Journal of Nuclear Energy, Part B: Reactor Technology, 1959, Vol. 1, pp. 123-129

13. Sukhatme, S.P., and W.M. Rohsenow, Heat Transfer During Film Condensation of a Liquid Metal Vapor, Third Annual High Temperature Liquid Metal Heat Transfer Meeting, Oak Ridge National Lab., Sept. 4-6, 1963, AEC Contract No. AT(30-1)-2995

14. Misra, B., and C.F. Bonilla, Chem. Eng. Progr. Symp. Vol. 52, No. 2, pp. 7-21, 1956

15. Chen, M.M., Trans. ASME, Journal of Heat Transfer 83, 48-60, 1961

16. Lee, J., Remarks on Liquid Metal Condensation, AIChE Paper 1, Seventh National Heat Transfer Conference, August 9-12, 1964

17. Alkali Metals Boiling and Condensing Investigations, Quarterly Progress Report 8, Edited by F.E. Tippets, NASA CR-54138, Oct. 20, 1964

18. van Driest, E.R., On Turbulent Flow Near a Wall, Journal Aeronautical Science, November 1956, pp. 1007-1011

19. Laufer, J., The Structure of Turbulence in Fully-Developed Pipe Flow, NACA Report 1174, 1954

20. Beckwith, W.F., and R. Fahien, Determination of Turbulent Thermal Diffusivities for Flow of Liquids in Pipes, Ames Laboratory IS-734, November 1963

21. Jenkins, R., Heat Transfer and Fluid Mechanics Institute, p. 147, Stanford University Press, 1951

22. Deissler, R. G., NACA Research Memo E52 F05, 1952

23. Lykoudis, P. A., and T. S. Touloukian, Trans. ASME, Vol. 80, No. 3, 653, 1958

24. Rohsenow, W. M. and S. Cohen, The Influence of the Ratio of Eddy Diffusivities on Heat Transfer to Liquid Metals, MIT Heat Transfer Lab Report, June 1960

25. Mizushina, T., and T. Sasano, Paper No. 78 presented at 1961 International Heat Transfer Conference, Boulder, Colorado

26. Azer, N. Z., and B. T. Chao, International Journal of Heat and Mass Transfer, Vol. 1, No. 1, 121, 1960

27. Dwyer, O. E., AIChE Journal, Vol. 9, No. 2, p. 261, March 1963

28. Sesonske, A., S. L. Schrock and E. H. Buyco, AIChe Preprint No. 25, Sixth National Heat Transfer Conference, Boston, Mass., August 1963

29. Subbotin, V. I., M. Kh. Ibragimov, M. N. Ivanovskii, M. N. Arnol'dov, and E. V. Nomofilov, Turbulent Heat Transfer in a Stream of Molten Metals, Soviet Journal of Atomic Energy, Vol. 10, No. 4, pp. 384-386, April 1961

30. Brown, H. E., B. H. Amstead and B. E. Short, Trans. Am. Soc. Mech. Engr., Vol. 79, No. 2, p. 279, 1957

31. Isakoff, E., and T. B. Drew, Heat and Momentum Transfer in Turbulent Flow of Mercury, General Discussion on Heat Transfer, Inst. Mech. Eng. and ASME, 1951, pp. 405-409

32. Lockhart, R. W., and R. C. Martinelli, Chem. Eng. Prog. Symp. Series, Vol. 45, No. 1, p. 39, 1949

33. Dukler, A. E., PhD. Thesis, Univ. of Delaware, 1951

34. Charvonia, D. A., A Study of the Mean Thickness of the Liquid Film and the Characteristics of the Interfacial Surface in Annular Two-Phase Flow in a Vertical Pipe, Jet Propulsion Center, Purdue University, Report Number I-59-1, May 1959

35. Chien, S. F., An Experimental Investigation of the Liquid Film
    Structure and Pressure Drop of Vertical, Downward Annular,
    Two-Phase Flow, PhD Thesis, University of Minnesota,
    April 1961

36. Collier, J. G., and G. F. Hewitt, Data on the Vertical Flow of
    Air-Water Mixtures in the Annular and Dispersed Flow
    Regions, Chemical Engineering Division, Atomic Energy
    Research Establishment, Harwell, Berkshire, England,
    Report AERE-R-3455, 1960

37. Carpenter, F., Heat Transfer and Pressure Drop for Condensing
    Pure Vapors Inside Vertical Tubes at High Vapor Velocities,
    PhD Thesis, Univ. of Delaware, 1948

38. Goodykoontz, J., and R. G. Dorsch, Unpublished Preliminary
    Data, NASA Lewis Research Center

39. Schlichting, H., Boundary Layer Theory, McGraw-Hill,
    New York, 1960

APPENDIX F

Figures

SKETCH OF ASSUMED FLOW MODEL

TUBE WALL

LIQUID FILM

MASS TRANSFER
AT INTERFACE

VAPOR CORE

DIRECTION
OF FLOW

VAPOR LIQUID
INTERFACE
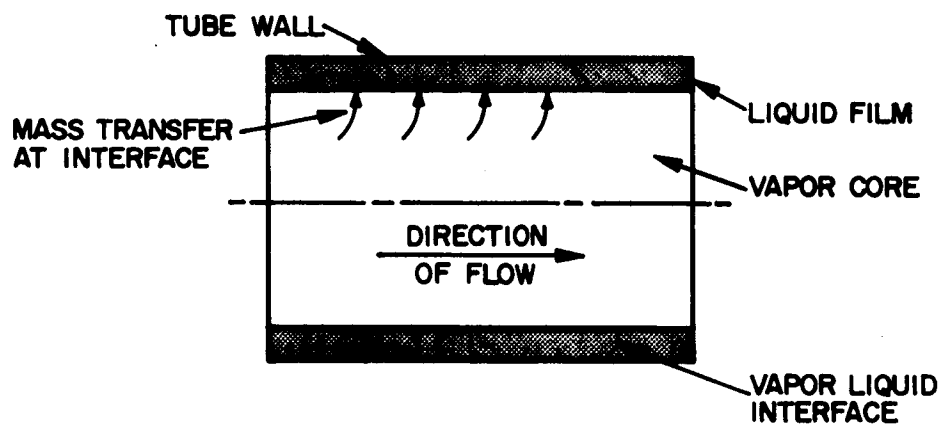
Figure 1

u⁺ vs y⁺ FOR FULLY-DEVELOPED PIPE FLOW
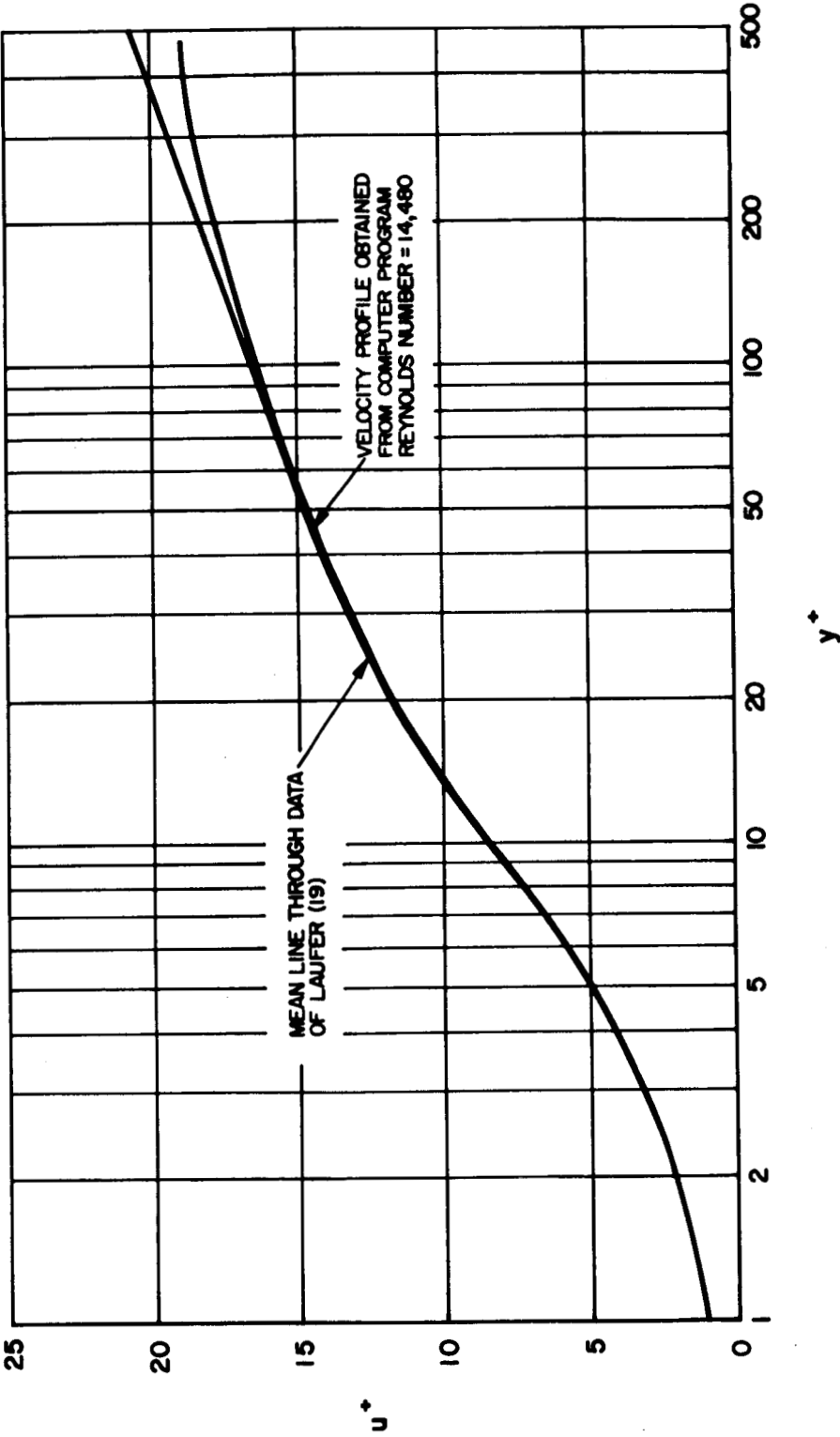
Figure 2

VARIATION OF τ/τ_0 AND ϵ_m/ν_L WITH y/r
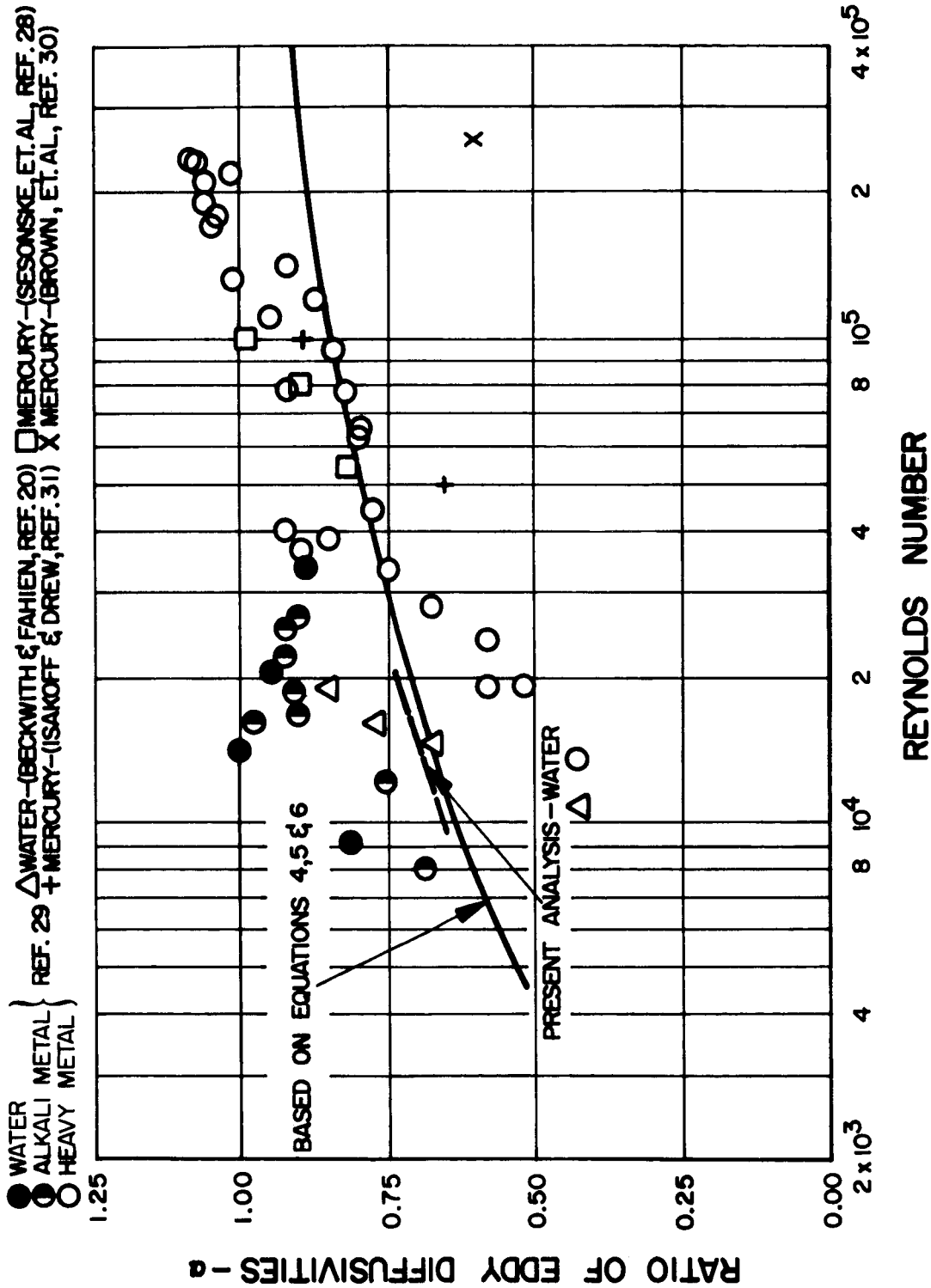## FOR FULLY-DEVELOPED PIPE FLOW
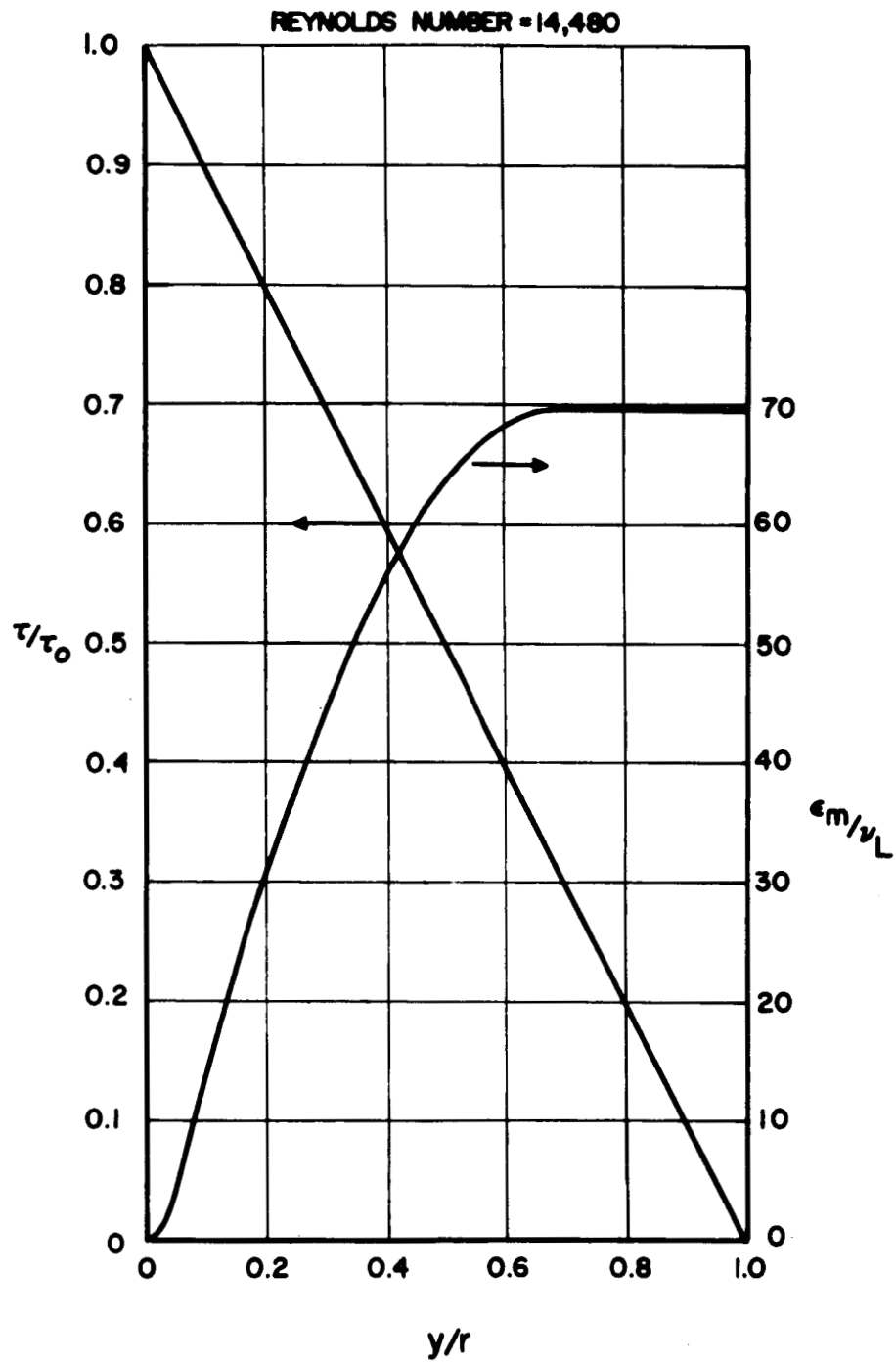
Figure 3

Figure 4

VARIATION OF RATIO OF EDDY DIFFUSIVITIES WITH y/r AND REYNOLDS NUMBER
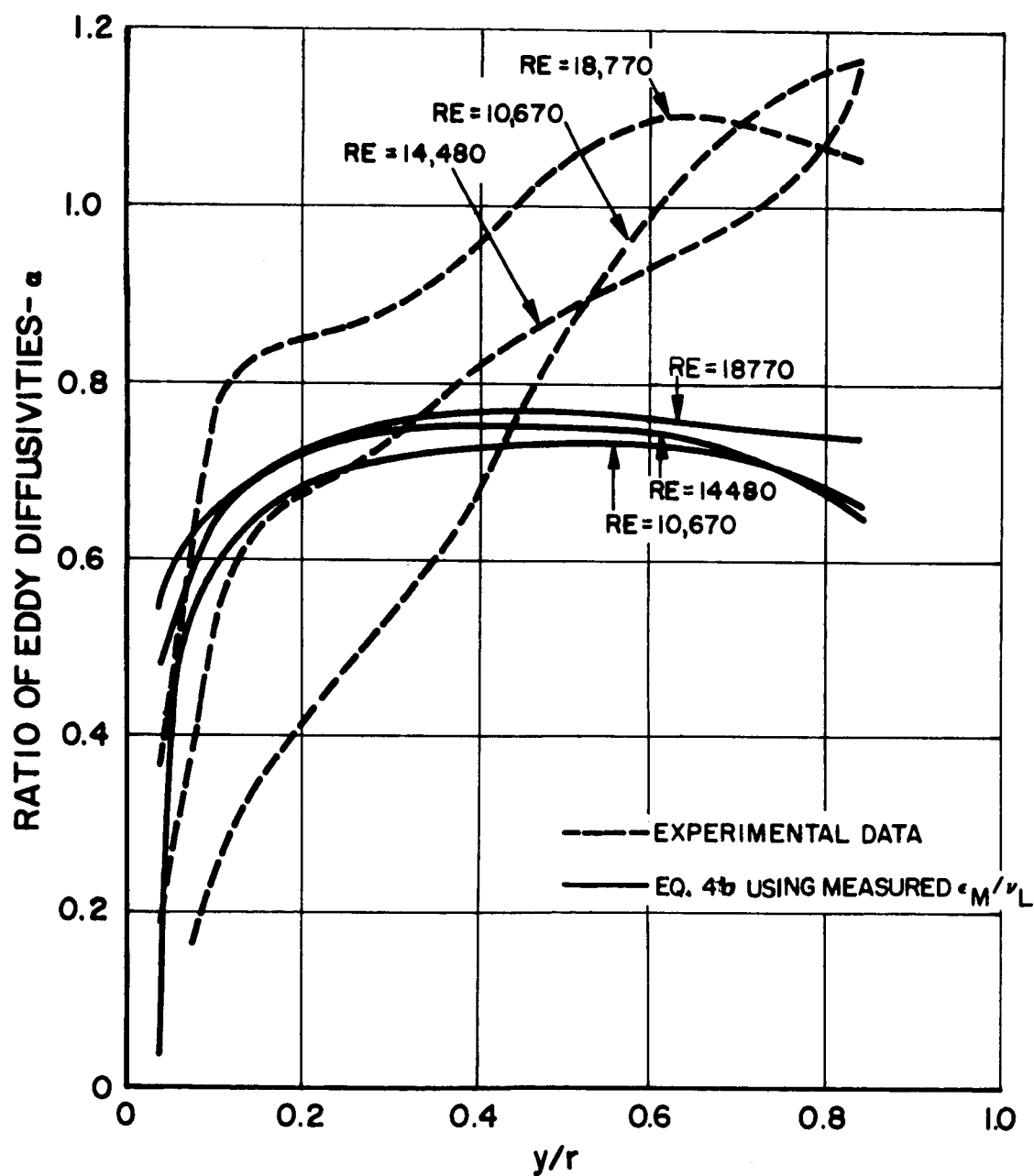
FROM DATA OF BECKWITH & FAHIEN (REF. 20)

Figure 5

VARIATION OF RATIO OF EDDY DIFFUSIVITIES WITH y/r AND REYNOLDS NUMBER

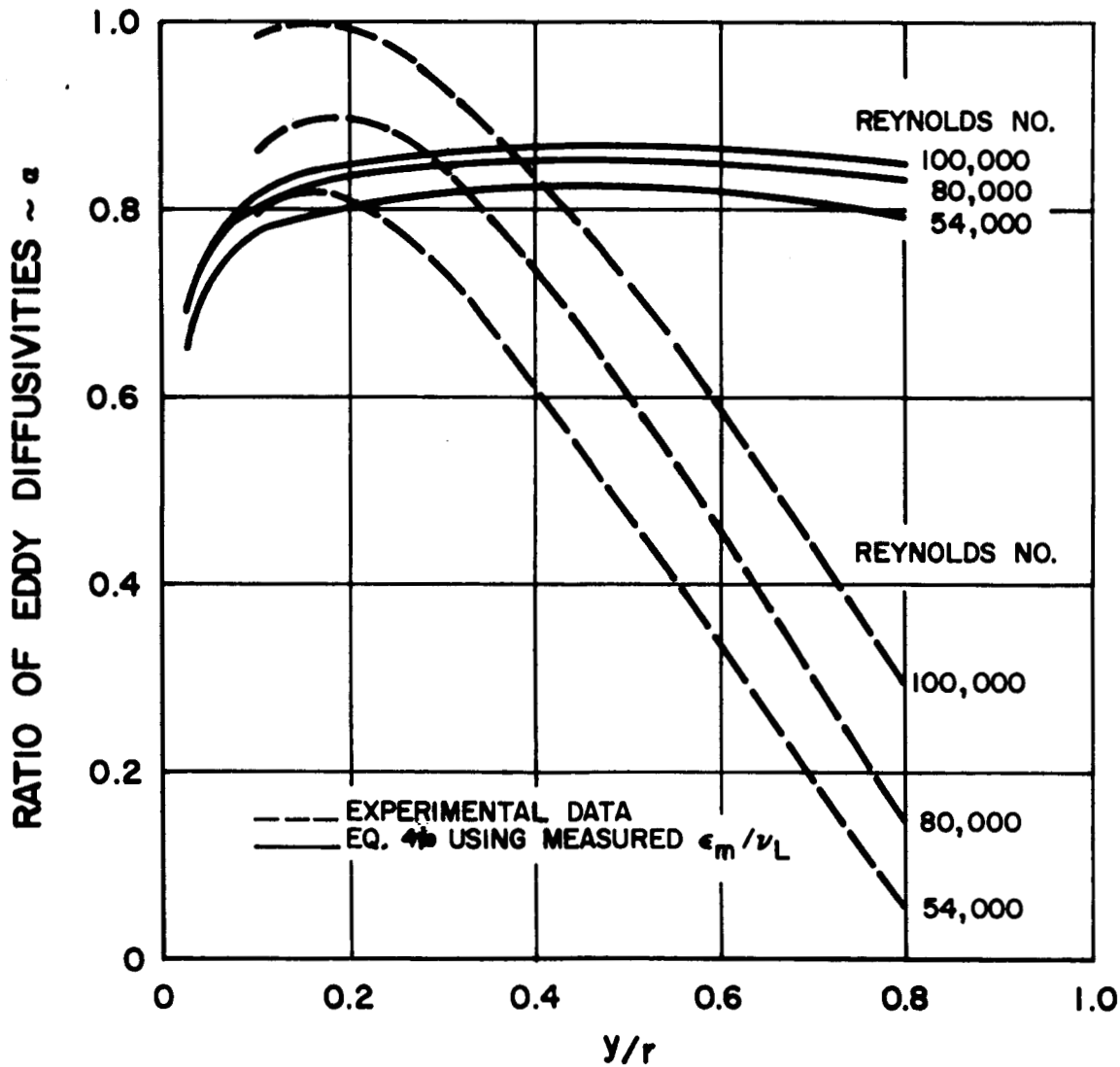## FROM DATA OF SESONSKE, ET AL (REF. 28)

Figure 6

CALCULATED FILM THICKNESS
vs MEASURED FILM THICKNESS
FOR CHARVONIA'S AND CHIEN'S DATA

$\frac{dP}{d\ell}$ BASED ON EXPERIMENTAL DATA

CONDITIONS
1. AIR-WATER MIXTURES
2. VERTICAL DOWNFLOW
3. PRESSURE ≈ 1 ATM
4. TEMPERATURE 55-85° F

▣ CHARVONIA (REF. 34)   TUBE I.D.=0.208 FT
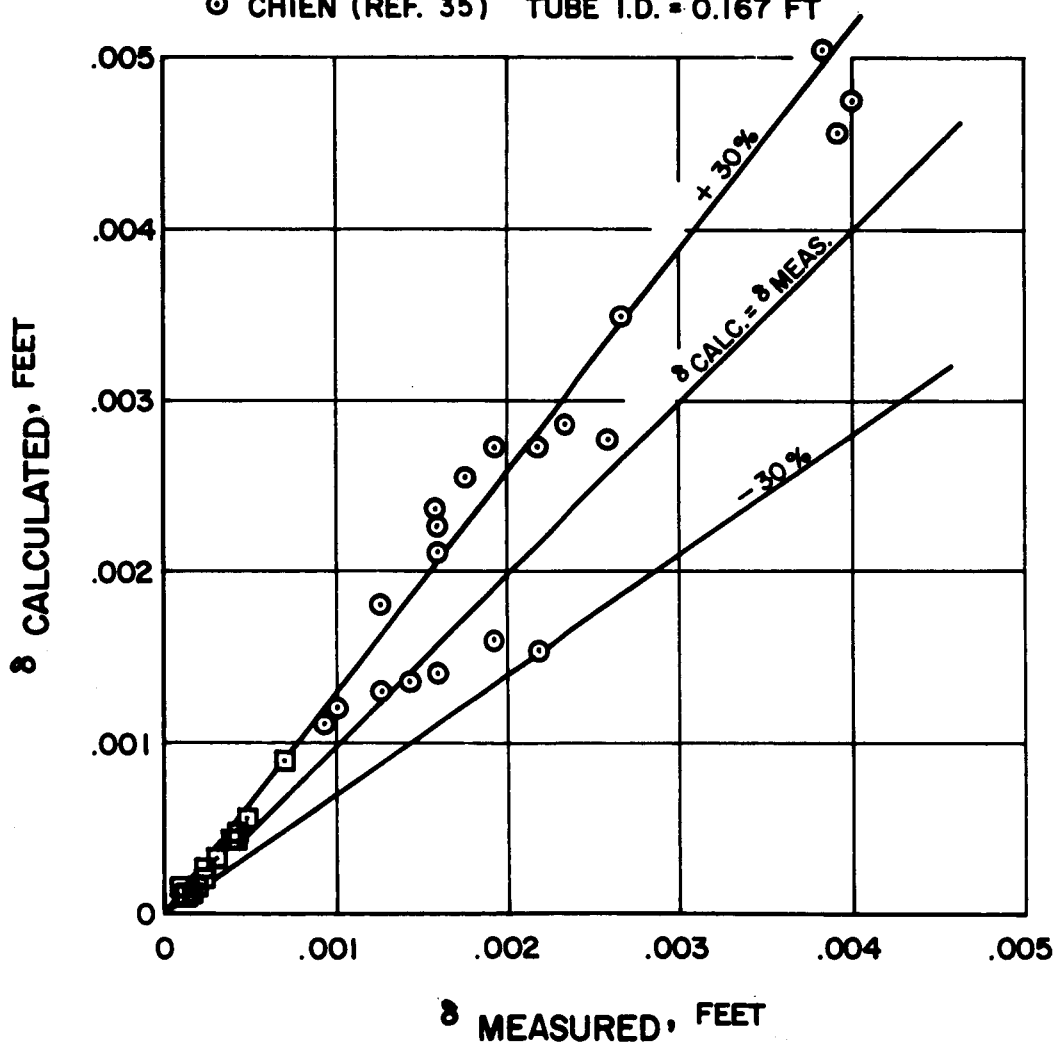
◎ CHIEN (REF. 35)   TUBE I.D.=0.167 FT

Figure 7

CALCULATED FILM THICKNESS
vs MEASURED FILM THICKNESS
FOR CHARVONIA'S AND CHIEN'S DATA

$\frac{dP}{d\ell}$ BASED ON DUKLER CORRELATION

CONDITIONS
1. AIR-WATER MIXTURES
2. VERTICAL DOWNFLOW
3. PRESSURE ≈ I ATM
4. TEMPERATURE 55-85°F

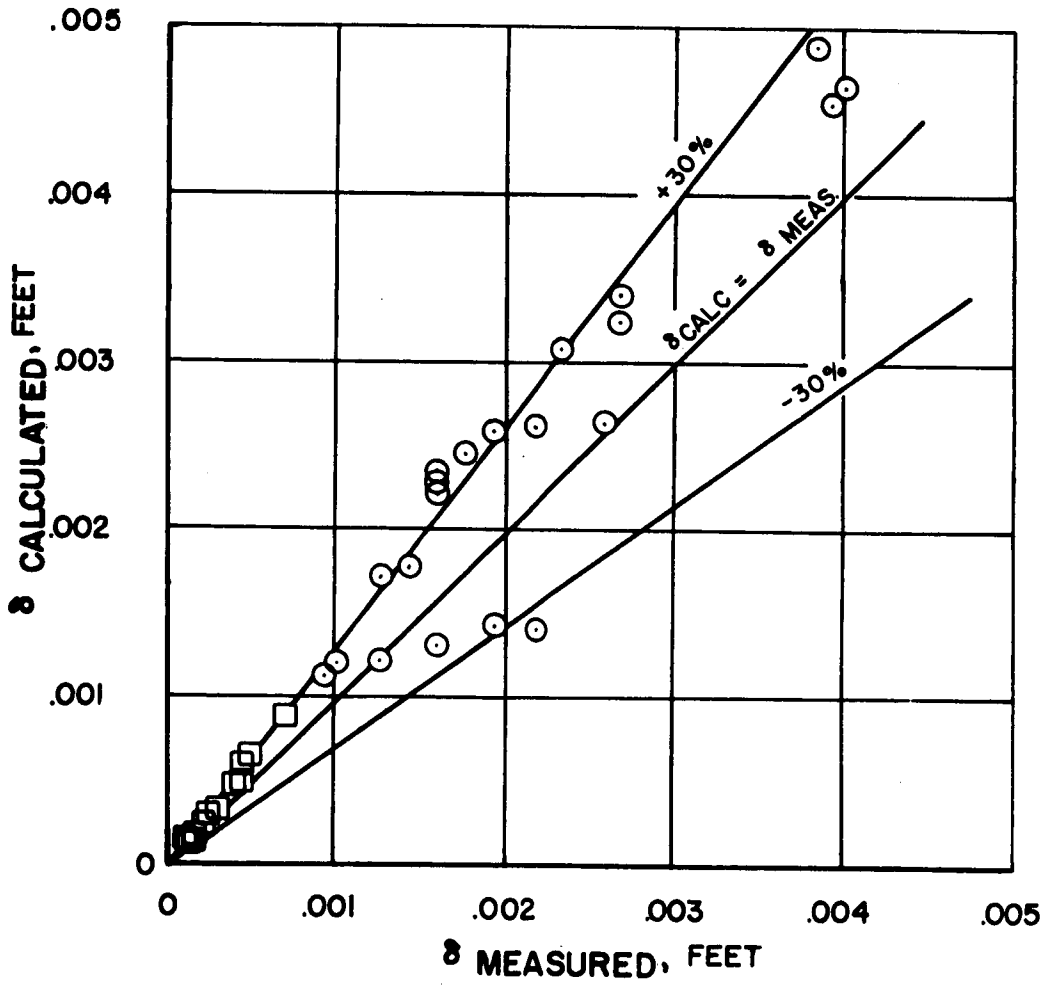□ CHARVONIA (REF. 34) TUBE ID = 0.208 FT

O CHIEN (REF. 35) TUBE ID = 0.167 FT

Figure 8.

CALCULATED FILM THICKNESS
vs MEASURED FILM THICKNESS
FOR CHARVONIA'S AND CHIEN'S DATA

$\frac{dP}{d\ell}$ BASED ON LOCKHART-MARTINELLI CORRELATION

CONDITIONS
1. AIR-WATER MIXTURES
2. VERTICAL DOWNFLOW
3. PRESSURE $\approx$ 1 ATM
4. TEMPERATURE 55-85°F

☐ CHARVONIA (REF. 34) TUBE I.D.=0.208 FT
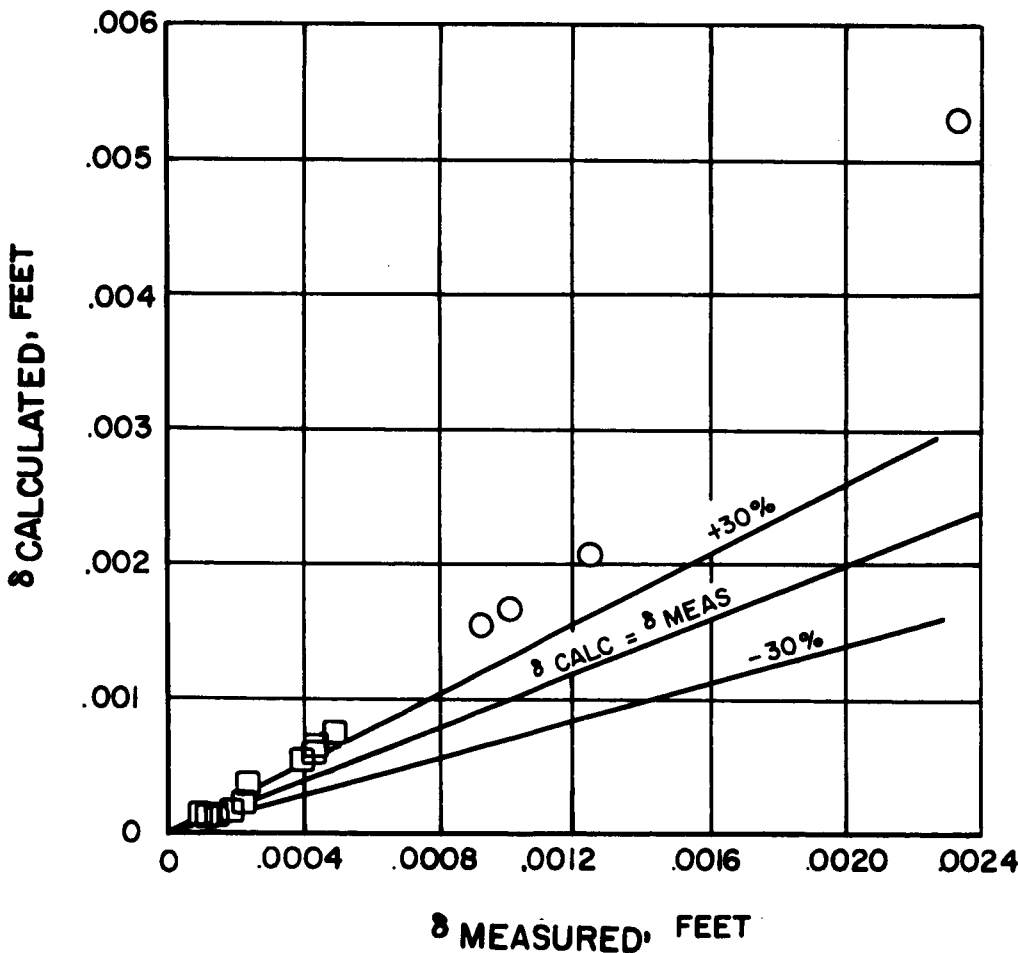
○ CHIEN (REF. 35) TUBE I.D.=0.167 FT

Figure 9

VARIATION OF FILM THICKNESS
WITH AIR AND WATER FLOW RATES

CONDITIONS
1. AIR-WATER MIXTURES
2. VERTICAL DOWNWARD FLOW
3. PRESSURE ≈ I ATM
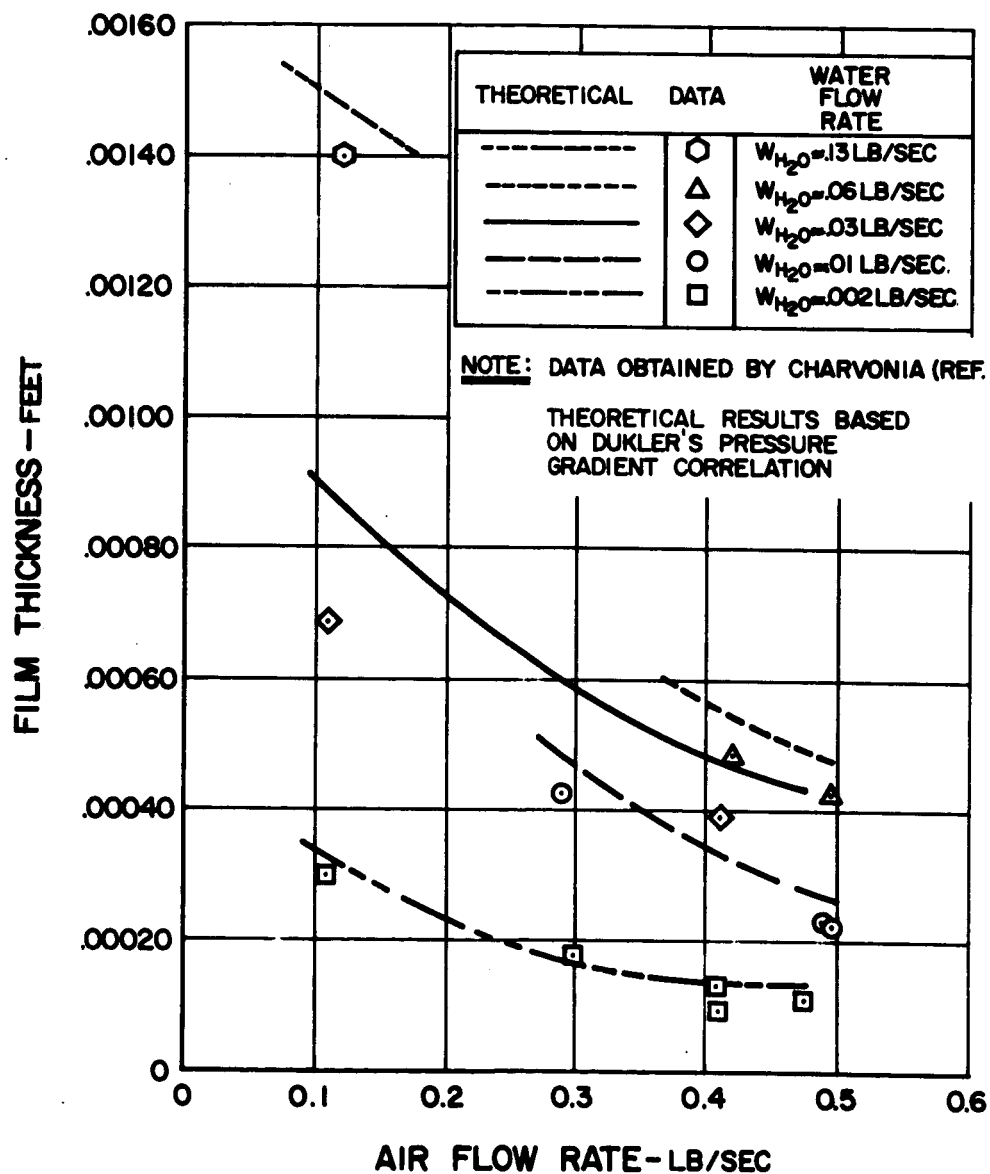4. TEMPERATURE = 55-80° F
5. TUBE I.D. = 0.208 FEET

THEORETICAL	DATA	WATER FLOW RATE
-------	⬡	W_{H_2O}=.13 LB/SEC
--------	△	W_{H_2O}=.06 LB/SEC
———	◇	W_{H_2O}=.03 LB/SEC
— — —	○	W_{H_2O}=.01 LB/SEC.
---------	▢	W_{H_2O}=.002 LB/SEC.

NOTE: DATA OBTAINED BY CHARVONIA (REF. 34.)

THEORETICAL RESULTS BASED
ON DUKLER'S PRESSURE
GRADIENT CORRELATION

Figure 10

VARIATION OF FILM THICKNESS
WITH AIR AND WATER FLOW RATES

CONDITIONS
1. AIR-WATER MIXTURES
2. VERTICAL DOWNWARD FLOW
3. PRESSURE ≈ 1 ATM
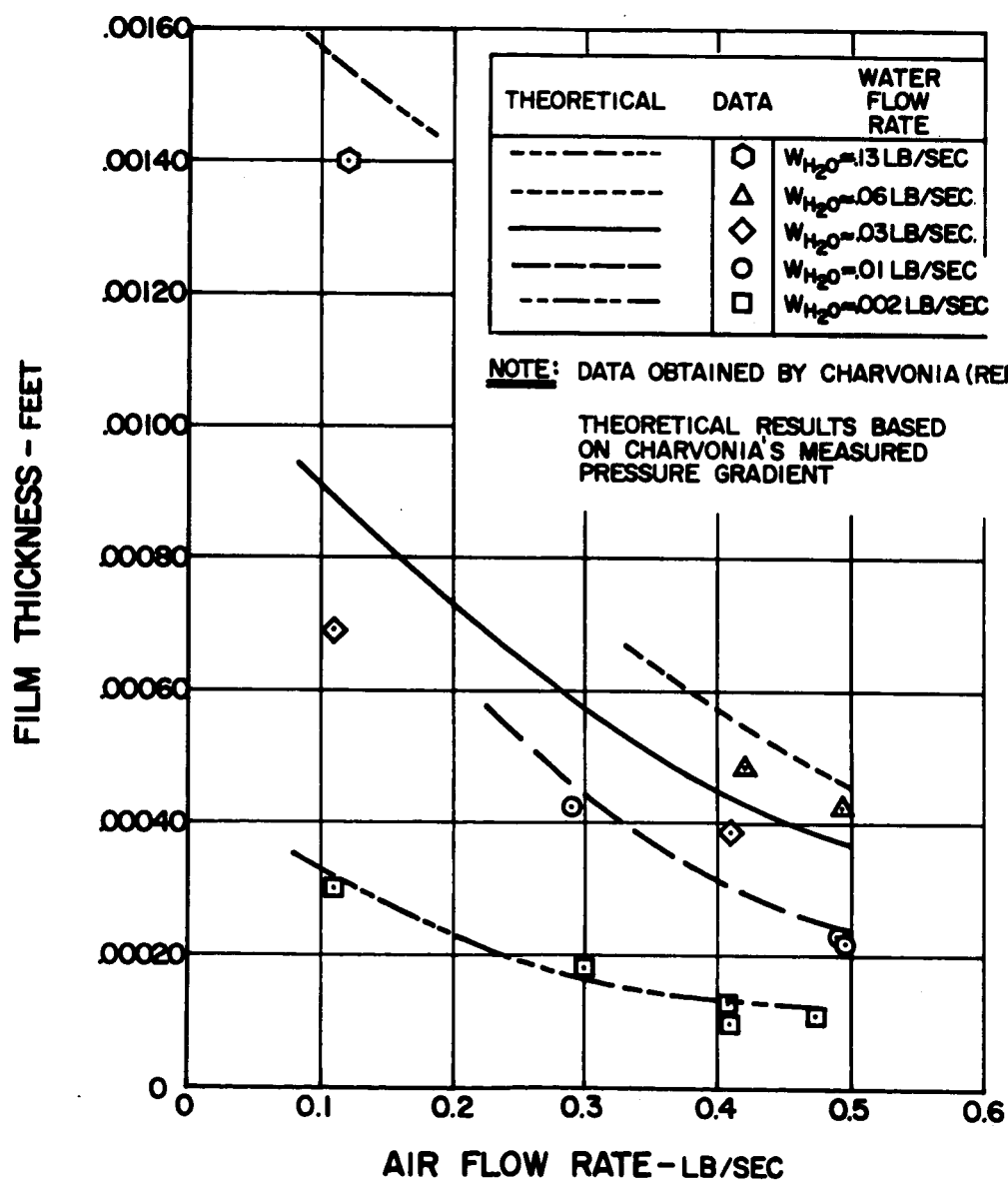4. TEMPERATURE = 55-80° F
5. TUBE I.D. = 0.208 FEET

THEORETICAL	DATA	WATER FLOW RATE
— — — — —	○	W_{H_2O}=.13 LB/SEC
— — — — —	△	W_{H_2O}=.06 LB/SEC.
———————	◇	W_{H_2O}=.03 LB/SEC.
— — — —	○	W_{H_2O}=.01 LB/SEC
— · — · —	□	W_{H_2O}=.002 LB/SEC

NOTE: DATA OBTAINED BY CHARVONIA (REF. 34)

THEORETICAL RESULTS BASED ON CHARVONIA'S MEASURED PRESSURE GRADIENT

FILM THICKNESS – FEET

AIR FLOW RATE–LB/SEC

Figure   11

CALCULATED FILM THICKNESS vs MEASURED FILM THICKNESS FOR COLLIER AND HEWITT DATA

$\frac{dP}{dL}$ BASED ON LOCKHART-MARTINELLI CORRELATION

CONDITIONS

1. AIR-WATER MIXTURE
2. VERTICAL UPFLOW
3. PRESSURE $\approx$ 1 ATM
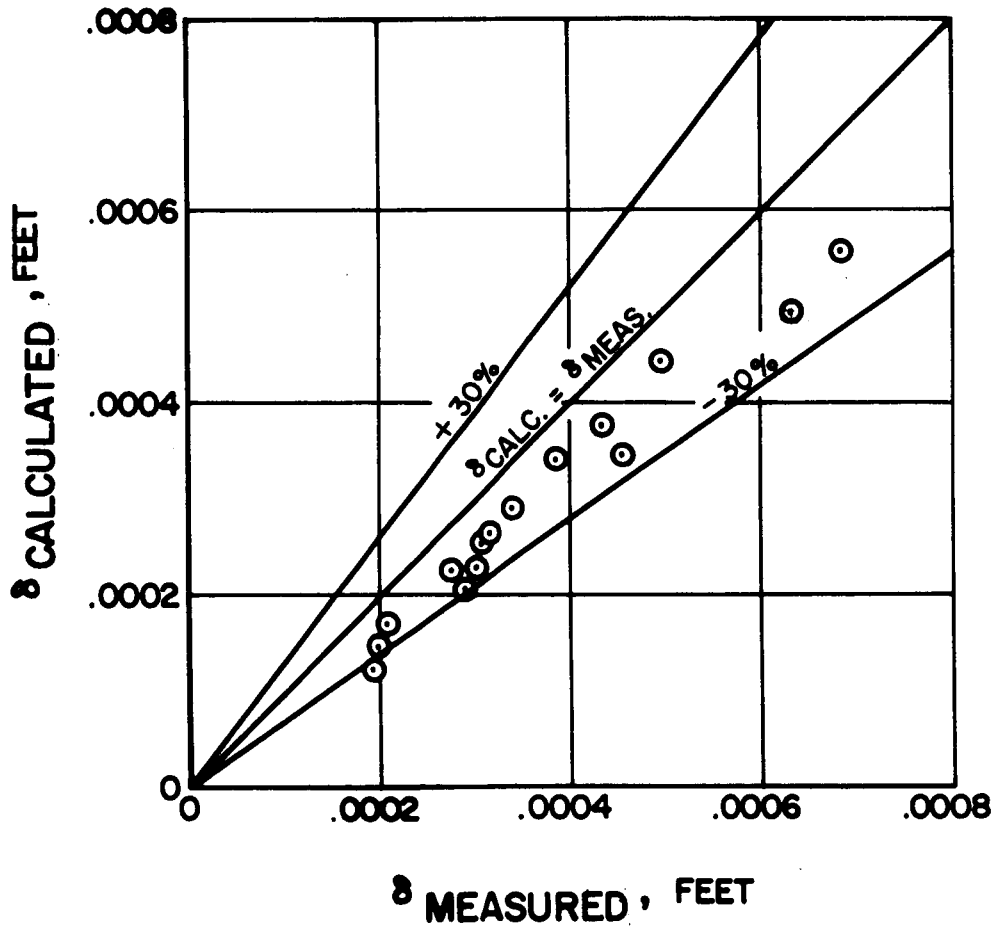4. TEMPERATURE $\approx$ 65° F
5. TUBE I.D. = .104 FT

Figure 12

EFFECT OF LIQUID SUBCOOLING ON PER CENT DIFFERENCE BETWEEN Wg/Wᴛ AND QUALITY BASED ON ENTHALPY

CONDITIONS

1. FLUID-WATER
2. VERTICAL DOWNFLOW
3. PRESSURE LEVEL ≈ 25 PSI
4. SATURATION TEMPERATURE ≈ 240° F
5. TUBE I.D. = 0.02445 FT
6. TOTAL FLOW RATE = 57.9 LB/HR

＊ NOTE: THESE CONDITIONS ARE THE SAME
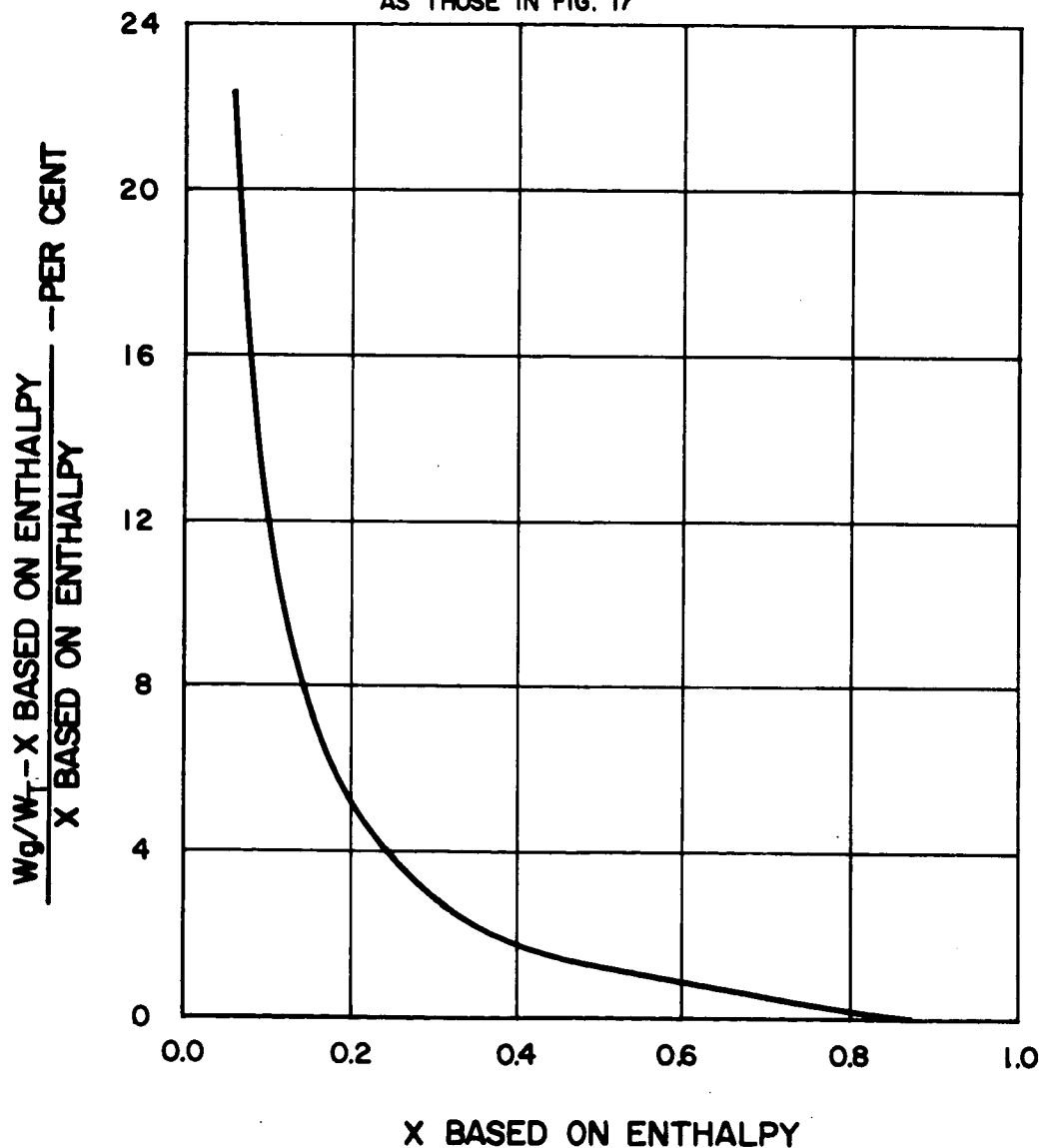AS THOSE IN FIG. 17

Figure 13

VARIATION OF HEAT TRANSFER COEFFICIENT WITH LIQUID VISCOSITY

CONDITIONS

1. FLUID-WATER
2. VERTICAL DOWNFLOW
3. PRESSURE = 16.8 PSIA
4. SATURATION TEMPERATURE = 219 °F
5. TUBE INSIDE DIAMETER=0.0382 FT
6. TOTAL FLOW=73.6 LB/HR
7. QUALITY =0.1276
8. HEAT FLUX DENSITY = 61,900 BTU/HR FT^2
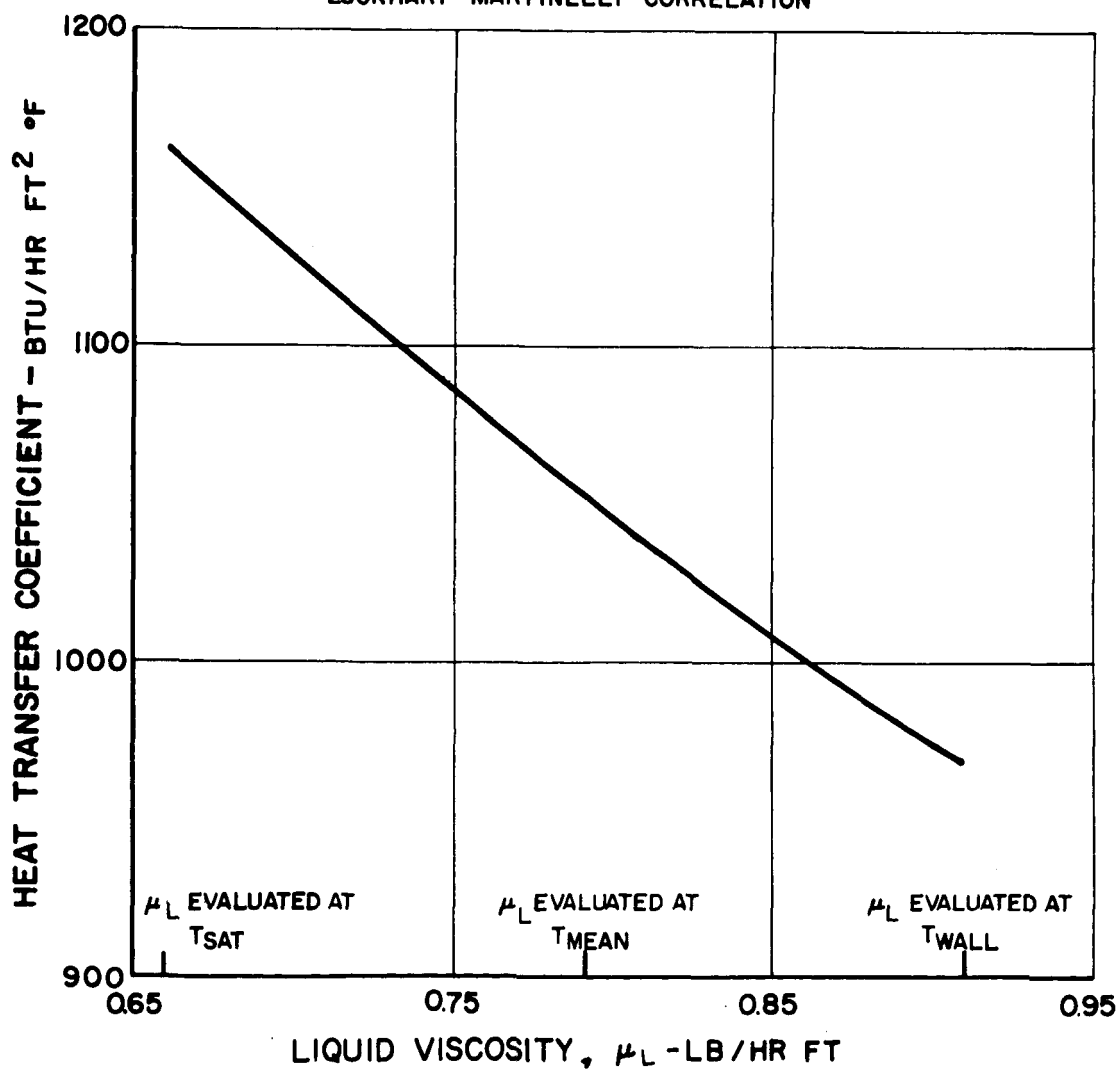9. FRICTIONAL PRESSURE GRADIENT BASED ON LOCKHART-MARTINELLI CORRELATION

Figure 14

CALCULATED HEAT TRANSFER COEFFICIENT vs EXPERIMENTAL HEAT TRANSFER COEFFICIENT. dP/dℓ BASED ON LOCKHART-MARTINELLI CORRELATION. α OBTAINED FROM EQ.4b

CONDITIONS

1. FLUID-WATER
2. VERTICAL DOWNFLOW
3. PRESSURE RANGE 16.8-25.0 PSIA
4. SATURATION TEMPERATURE RANGE 219-240°F
5. AVERAGE MASS VELOCITY RANGE 9,800-110,000 LB/HR FT^2

Figure 15

CALCULATED HEAT TRANSFER COEFFICIENT vs EXPERIMENTAL HEAT TRANSFER COEFFICIENT.
dp/dℓ BASED ON DUKLER CORRELATION
α OBTAINED FROM EQ. 4b

CONDITIONS

1. FLUID-WATER
2. VERTICAL DOWNFLOW
3. PRESSURE RANGE 16.8-25.0 PSIA
4. SATURATION TEMPERATURE RANGE 219-240°F
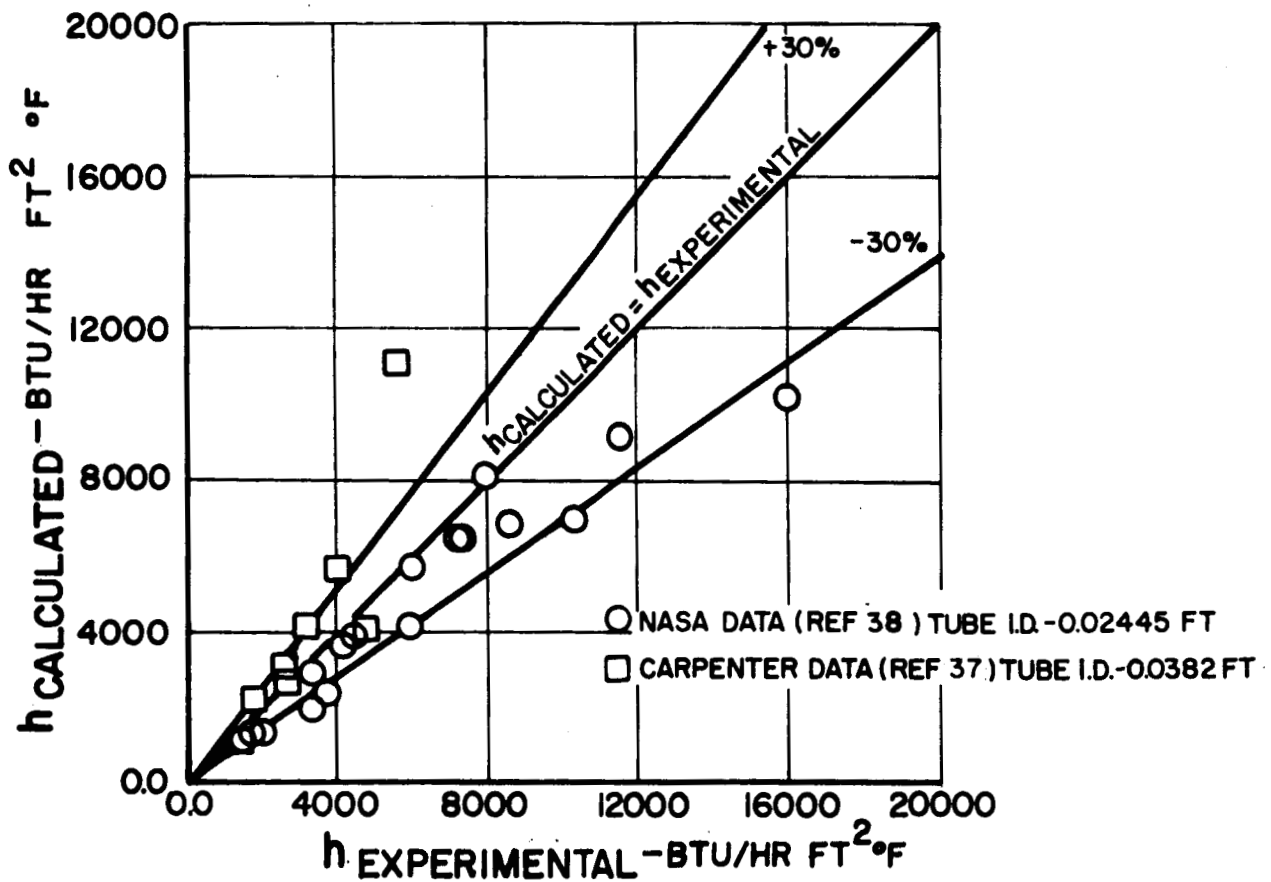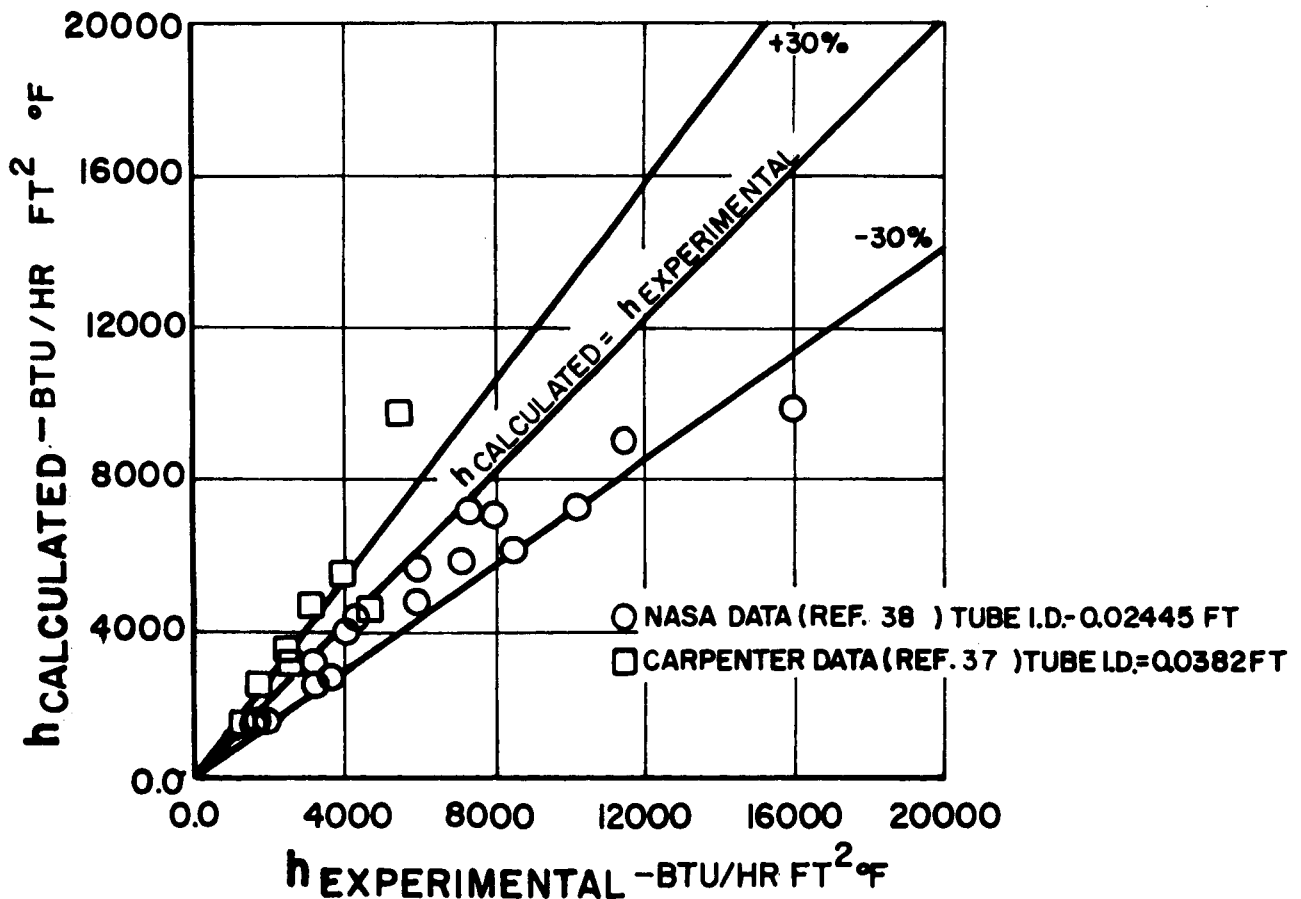5. AVERAGE MASS VELOCITY RANGE 9,800-110,000 LB/HR FT^2

Figure 16

EXPERIMENTAL AND CALCULATED HEAT TRANSFER COEFFICIENTS vs QUALITY. NASA DATA (REF. 38)

CONDITIONS
1. FLUID—WATER
2. VERTICAL DOWNFLOW
3. PRESSURE LEVEL ≈ 25 PSIA
4. SATURATION TEMPERATURE ≈ 240° F
5. TUBE I.D. = 0.02445 FT
6. TOTAL FLOW RATE = 57.9 LB/HR
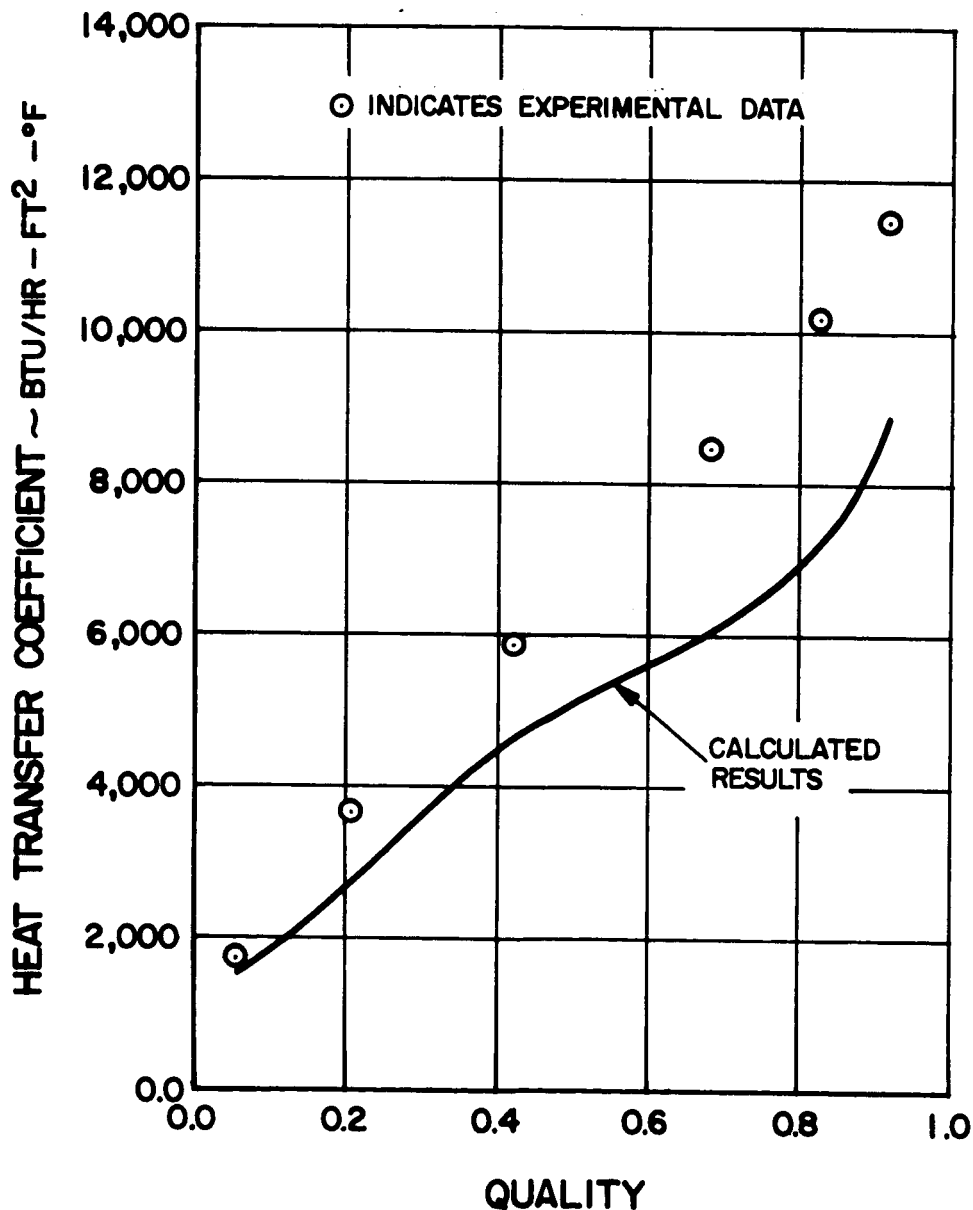7. dP/d𝑙 BASED ON DUKLER CORRELATION

Figure 17

EXPERIMENTAL AND CALCULATED HEAT TRANSFER COEFFICIENTS vs QUALITY CARPENTER DATA (REF. 37)

CONDITIONS

1. FLUID-WATER
2. VERTICAL DOWNFLOW
3. PRESSURE LEVEL ≅ 16.8 PSIA
4. SATURATION TEMPERATURE ≅ 219°F
5. TUBE I.D. = 0.0382 FT
6. TOTAL FLOW RATE = 72.4 LB/HR
7. dP/dl BASED ON DUKLER CORRELATION
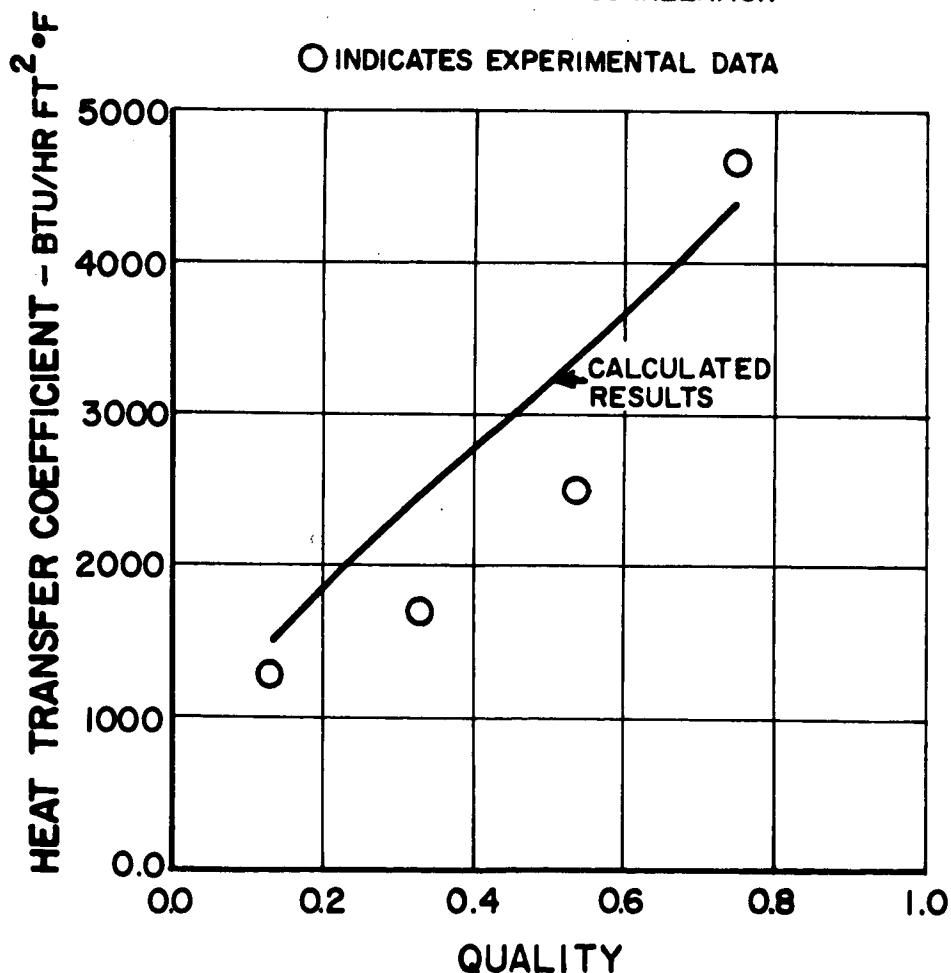
O INDICATES EXPERIMENTAL DATA

Figure 18

CALCULATED HEAT TRANSFER COEFFICIENT vs EXPERIMENTAL HEAT TRANSFER COEFFICIENT. dP/dℓ BASED ON LOCKHART-MARTINELLI CORRELATION. $\alpha = 1.0$

CONDITIONS

1. FLUID-WATER
2. VERTICAL DOWNFLOW
3. PRESSURE RANGE 16.8-25.0 PSIA
4. SATURATION TEMPERATURE RANGE 219-240°F
5. AVERAGE MASS VELOCITY RANGE 9,800-110,000 LB/HR FT^2

Figure 19

CALCULATED HEAT TRANSFER COEFFICIENT vs EXPERIMENTAL HEAT TRANSFER COEFFICIENT dp/dl BASED ON DUKLER CORRELATION

$\alpha = 1.0$

CONDITIONS

1. FLUID-WATER
2. VERTICAL DOWNFLOW
3. PRESSURE RANGE 16.8-25.0 PSIA
4. SATURATION TEMPERATURE RANGE 219-240°F
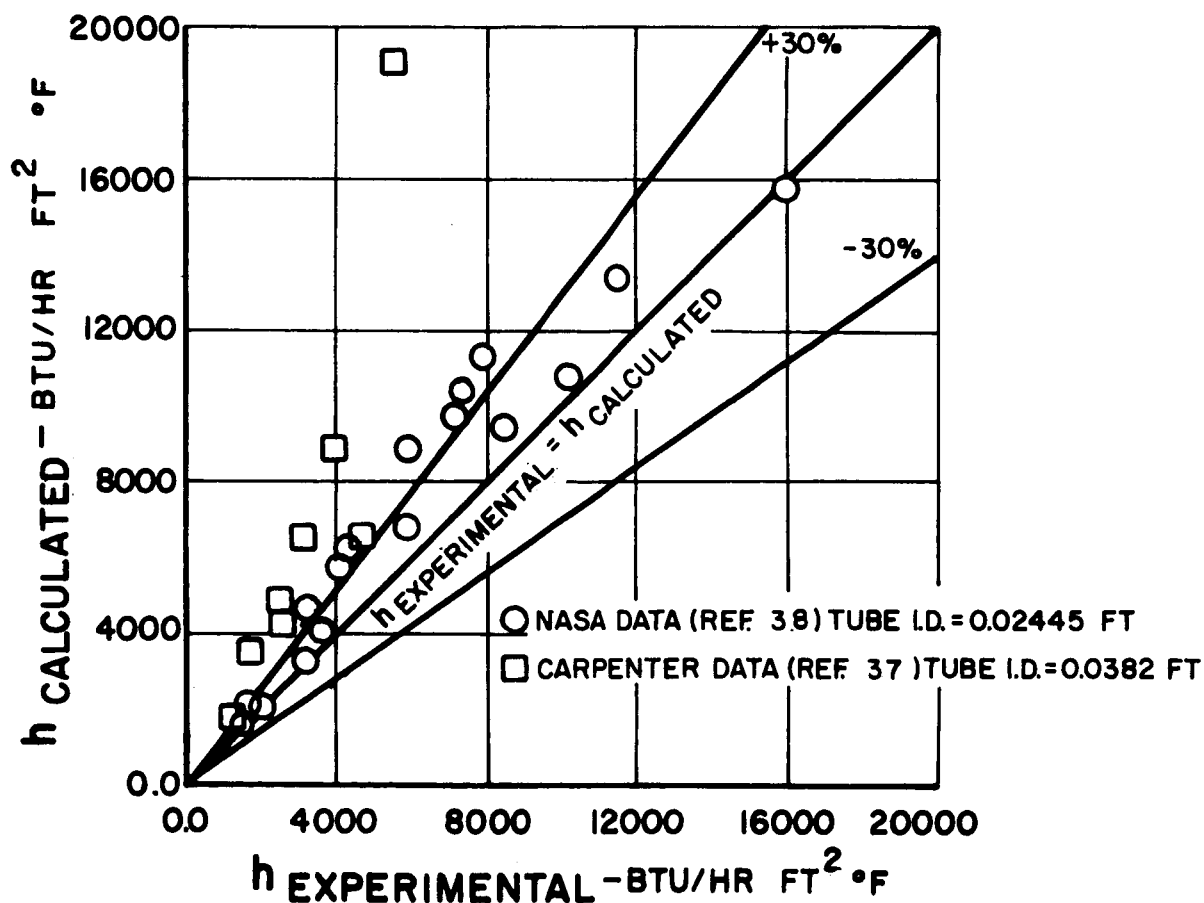5. AVERAGE MASS VELOCITY RANGE 9,800-110,000 LB/HR FT^2
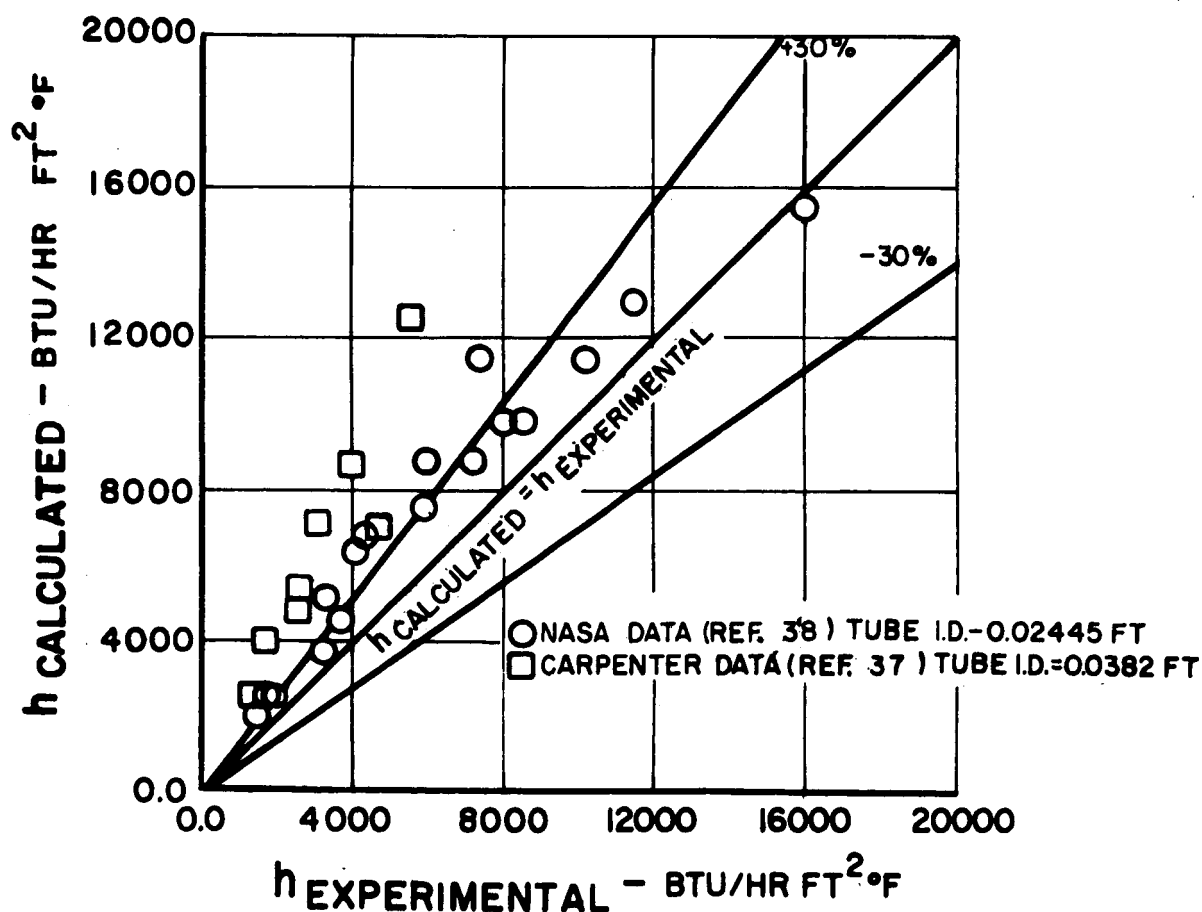
Figure 20

VARIATION OF u⁺ AND t⁺ WITH y⁺ FOR A LOW QUALITY CONDENSING WATER POINT
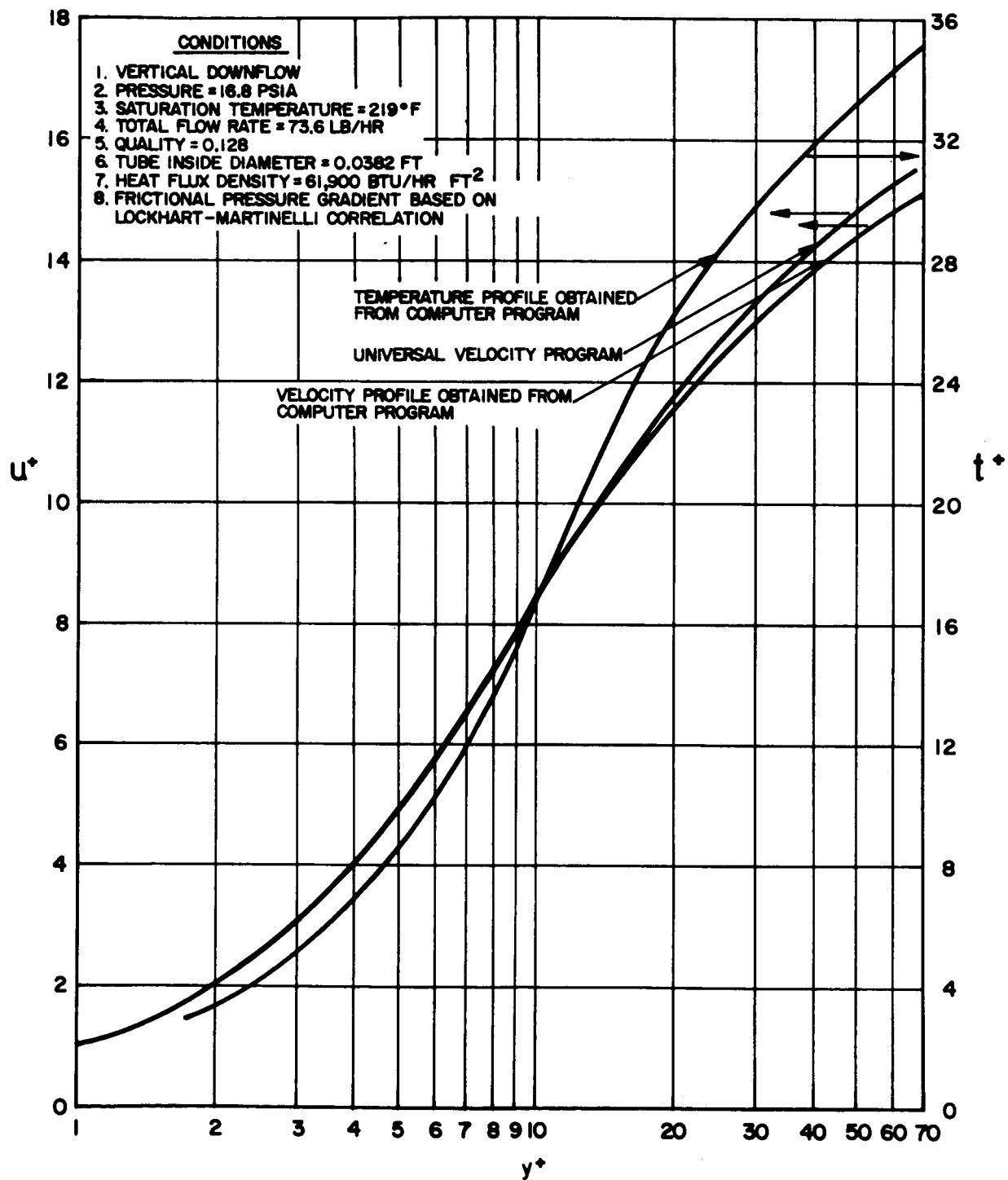
Figure 21

VARIATION OF τ/τ_0, ϵ_M/ν_L, α, AND $\epsilon_H/\left[\kappa_L/\rho_L C_{P_L}\right]$

WITH y/r FOR A LOW QUALITY CONDENSING WATER POINT

CONDITIONS

1. VERTICAL DOWNFLOW
2. PRESSURE = 16.8 PSIA
3. SATURATION TEMPERATURE = 219°F
4. TOTAL FLOW RATE = 73.6 LB/HR
5. QUALITY = 0.128
6. TUBE INSIDE DIAMETER = 0.0382
7. HEAT FLUX DENSITY = 61,900 BTU/HR FT^2
8. FRICTIONAL PRESSURE GRADIENT BASED ON
   LOCKHART-MARTINELLI CORRELATION
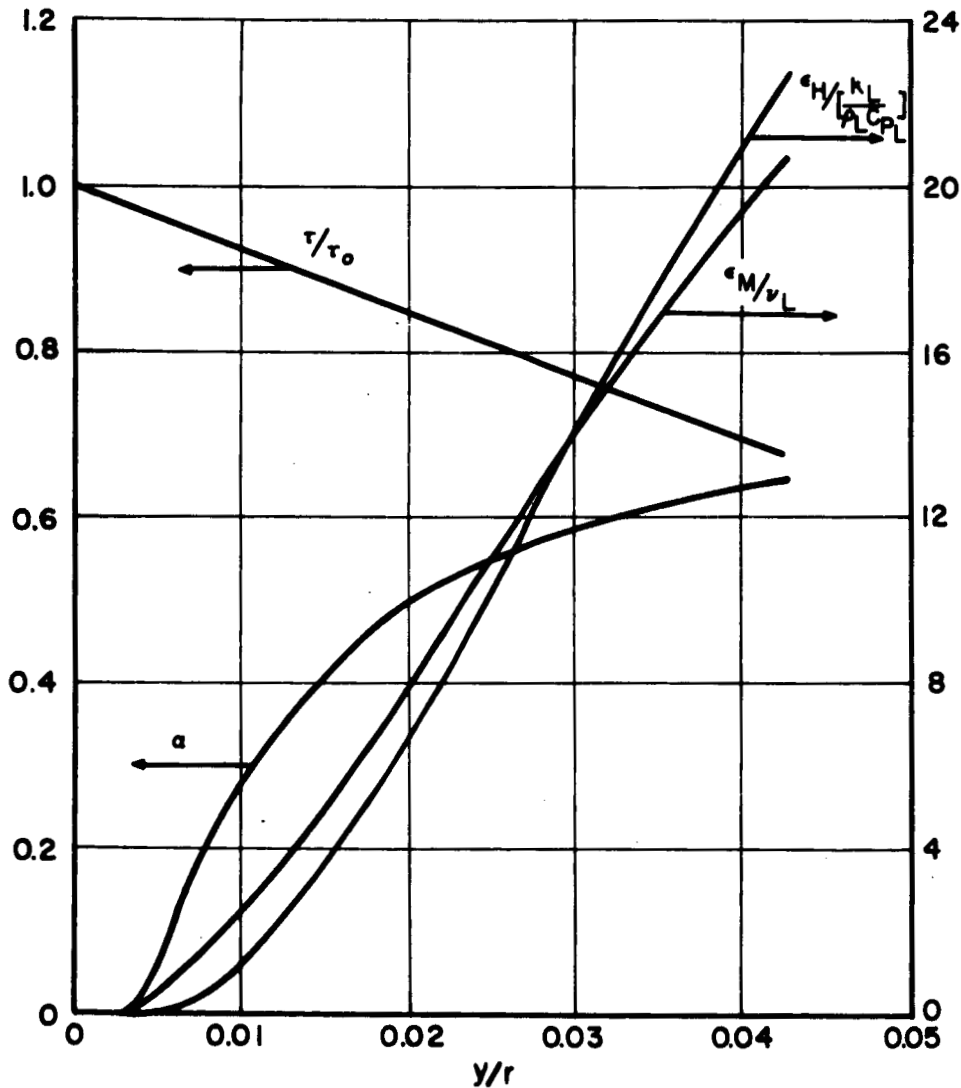
Figure 22

THEORETICAL HEAT TRANSFER COEFFICIENTS
FOR CONDENSING POTASSIUM vs QUALITY

SHOWING EFFECT OF TOTAL FLOW RATE

CONDITIONS:
1. VERTICAL DOWNFLOW
2. PRESSURE = 6.6 PSIA
3. SATURATION TEMPERATURE = 1250° F
4. TUBE INSIDE DIAMETER = 0.05208 FT
5. HEAT FLUX DENSITY = 60,000 BTU/HR FT^2
6. ASSUMING NO LIQUID–VAPOR INTERFACIAL RESISTANCE
7. FRICTIONAL PRESSURE GRADIENT BASED ON LOCKHART–MARTINELLI CORRELATION

TOTAL FLOW 80 LBS/HR
TOTAL FLOW 40 LBS/HR
TOTAL FLOW 20 LBS/HR

QUALITY

HEAT TRANSFER COEFFICIENT ~ BTU/HR FT^2 °F

Figure 23

THEORETICAL HEAT TRANSFER COEFFICIENTS
FOR CONDENSING POTASSIUM vs QUALITY
SHOWING EFFECT OF LIQUID-VAPOR INTERFACIAL RESISTANCE

CONDITIONS
1. VERTICAL DOWNFLOW
2. PRESSURE = 6.6 PSIA
3. SATURATION TEMPERATURE = 1250°F
4. TUBE INSIDE DIAMETER = 0.05208 FT
5. TOTAL FLOW = 40 LB/HR
6. HEAT FLUX DENSITY = 60,000 BTU/HR FT^2
7. FRICTIONAL PRESSURE GRADIENT BASED
   ON LOCKHART-MARTINELLI CORRELATION
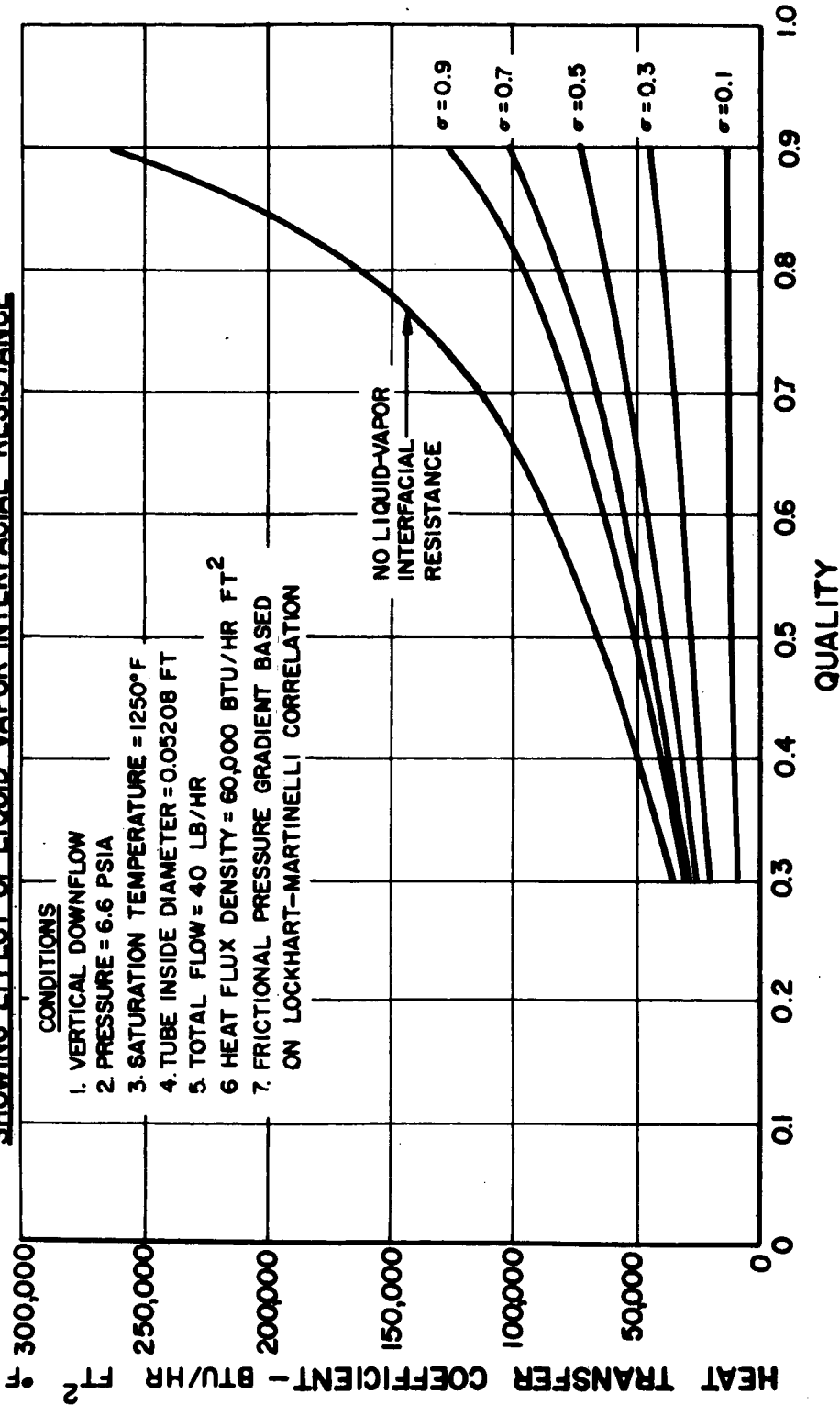
Figure 24

THEORETICAL HEAT TRANSFER COEFFICIENTS FOR CONDENSING POTASSIUM vs QUALITY

SHOWING EFFECT OF FRICTIONAL PRESSURE GRADIENT

$\left.\dfrac{dP}{dL}\right)_{fr}$ = TWICE THE LOCKHART-MARTINELLI VALUES

$\left.\dfrac{dP}{dL}\right)_{fr}$ OBTAINED FROM THE LOCKHART-MARTINELLI CORRELATION

$\left.\dfrac{dP}{dL}\right)_{fr}$ = HALF THE LOCKHART-MARTINELLI VALUES

CONDITIONS
1. VERTICAL DOWNFLOW
2. PRESSURE = 6.6 PSIA
3. SATURATION TEMPERATURE = 1250°F
4. TUBE INSIDE DIAMETER = 0.05208 FT
5. TOTAL FLOW = 40 LBS/HR
6. HEAT FLUX DENSITY = 60,000 BTU/HR FT²
7. ASSUMING NO LIQUID-VAPOR INTERFACIAL RESISTANCE

QUALITY

HEAT TRANSFER COEFFICIENT ~ BTU/HR FT² °F

Figure 25

VARIATION OF u⁺ AND t⁺ WITH y⁺ FOR CONDENSING POTASSIUM

CONDITIONS
1. VERTICAL DOWNFLOW
2. PRESSURE = 6.6 PSIA
3. SATURATION TEMPERATURE = 1250°F
4. TOTAL FLOW RATE = 40 LB/HR
5. QUALITY = 0.50
6. TUBE INSIDE DIAMETER = 0.05208 FT
7. HEAT FLUX DENSITY = 60,000 BTU/HR FT²
8. FRICTIONAL PRESSURE GRADIENT BASED ON
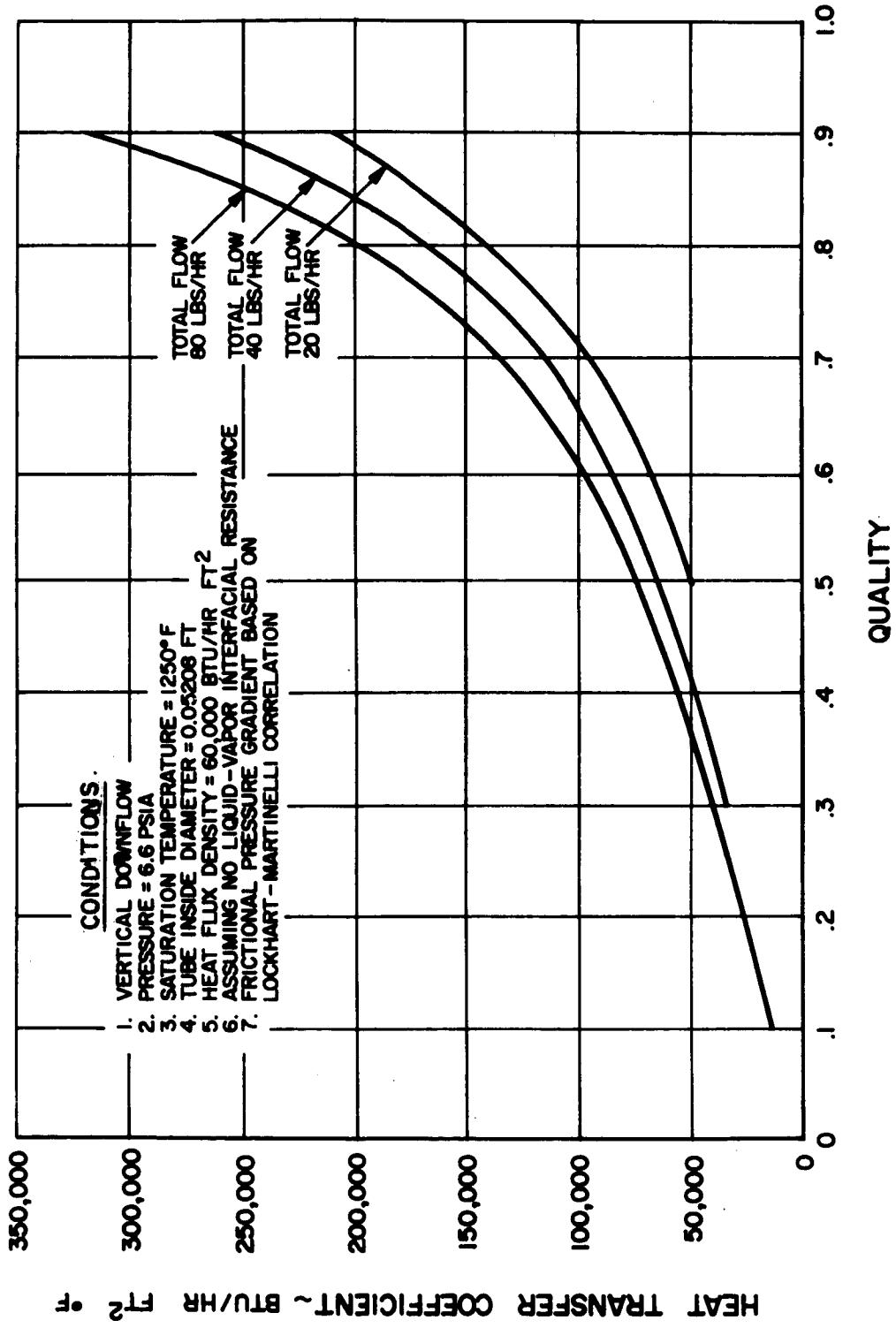   LOCKHART-MARTINELLI CORRELATION
9. NO LIQUID-VAPOR INTERFACIAL RESISTANCE
   ASSUMED

UNIVERSAL VELOCITY PROFILE

VELOCITY PROFILE OBTAINED FROM COMPUTER PROGRAM

TEMPERATURE PROFILE OBTAINED FROM COMPUTER PROGRAM

Figure 26

VARIATION OF τ/τ_0, ϵ_M/ν_L, α AND $\epsilon_H / \left[\dfrac{k_L}{\rho_L c_{P_L}}\right]$

WITH Y/r FOR CONDENSING POTASSIUM

CONDITIONS
1. VERTICAL DOWNFLOW
2. PRESSURE = 6.6 PSIA
3. SATURATION TEMPERATURE = 1250°F
4. TOTAL FLOW RATE = 40 LB/HR
5. QUALITY = 0.50
6. TUBE INSIDE DIAMETER = 0.05208 FT
7. HEAT FLUX DENSITY = 60,000 BTU/HR FT^2
8. FRICTIONAL PRESSURE GRADIENT BASED ON LOCKHART-MARTINELLI CORRELATION
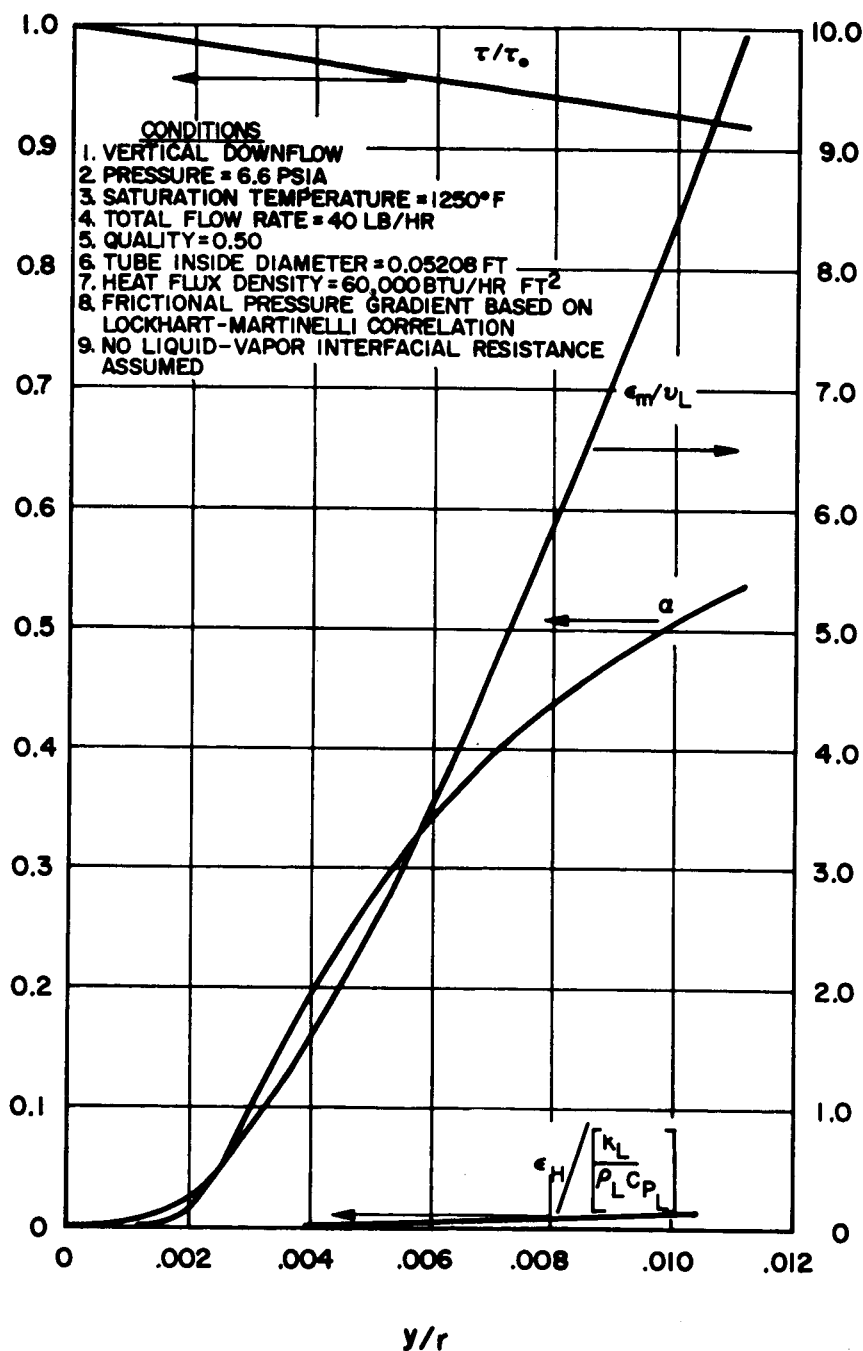9. NO LIQUID-VAPOR INTERFACIAL RESISTANCE ASSUMED

Figure 27

CONDENSING HEAT TRANSFER PARAMETER vs FILM REYNOLDS NUMBER SHOWING EFFECT OF LIQUID-VAPOR INTERFACIAL RESISTANCE

CONDITIONS
1. VERTICAL DOWNFLOW
2. PRESSURE = 6.6 PSIA
3. SATURATION TEMPERATURE = 1250°F
4. TOTAL FLOW RATE = 40 LB/HR
5. QUALITY = 0.3 - 0.9
6. TUBE INSIDE DIAMETER = 0.05208 FT
7. HEAT FLUX DENSITY = 60,000 BTU/HR FT²
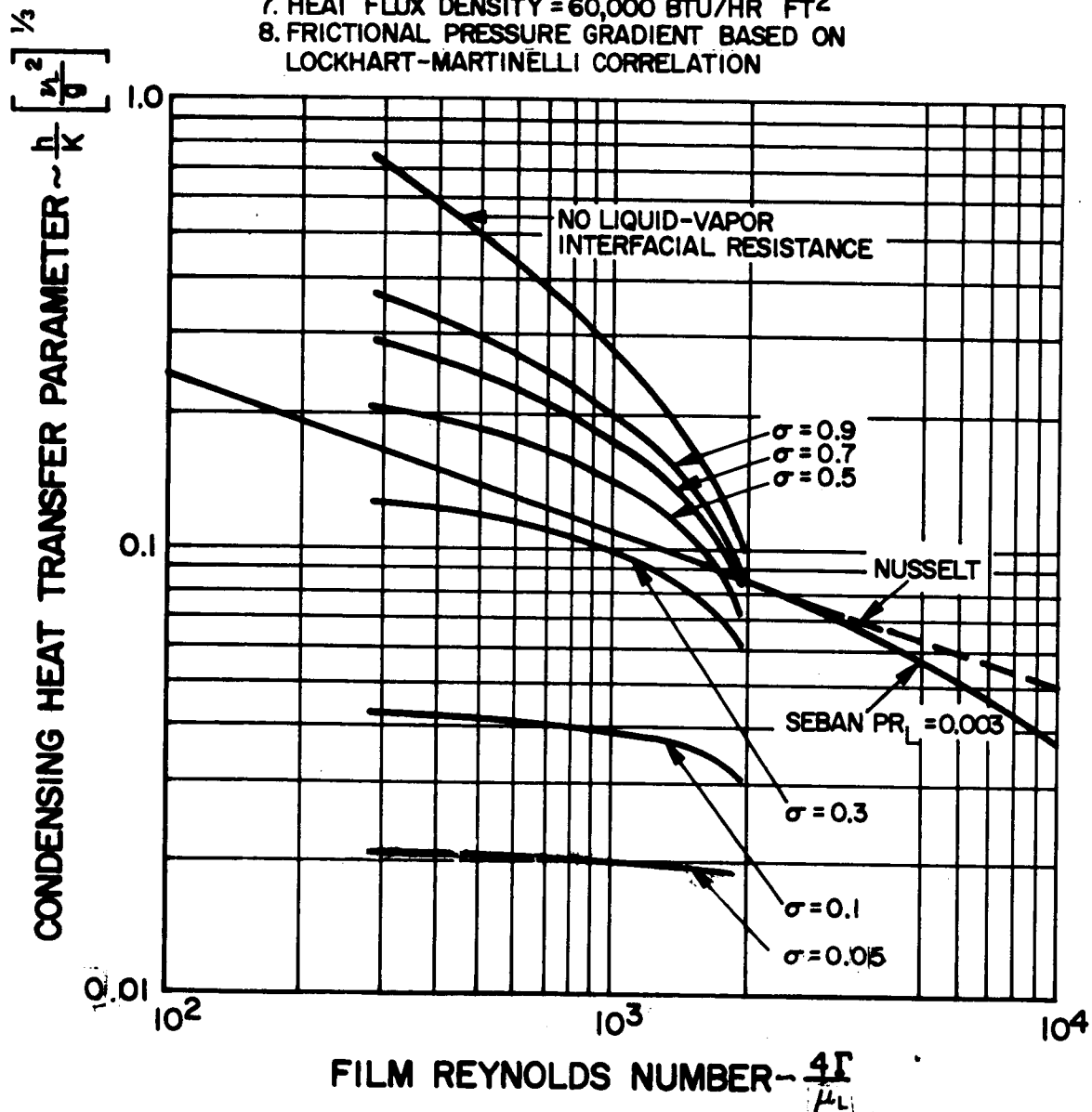8. FRICTIONAL PRESSURE GRADIENT BASED ON LOCKHART-MARTINELLI CORRELATION

Figure 28